Hindawi
Adsorption Science & Technology
Volume 2022, Article ID 4129833, 23 pages
https://doi.org/10.1155/2022/4129833

Research Article

Surface-Modified Adsorbent from *Artocarpus heterophyllus Lam* Biomass to Confine Reactive Red 194 in Real and Synthetic Effluents: Kinetics and Equilibrium Study

Lavanya Ramasamy and Lima Rose Miranda

Carbon Research and Engineering Laboratory, Department of Chemical Engineering, A.C. Tech, Anna University, Chennai-25, India

Correspondence should be addressed to Lima Rose Miranda; limamiranda2007@gmail.com

Received 27 December 2021; Revised 21 February 2022; Accepted 7 March 2022; Published 16 April 2022

Academic Editor: Ming Hua

Chemical activation of *Artocarpus heterophyllus Lam* (jackfruit peel) via phosphoric acid was focused on this study for the preparation of activated carbon. Carbonization was done at a temperature of 400°C based on the nature of biomass after the impregnation ratio of 1 : 1 (weight of phosphoric acid/weight of raw material). Titanium dioxide was doped on the prepared activated carbon through the sol-gel method. Titanium dioxide doped activated carbon was synthesized to perceive the nature of adsorbents under ambient conditions. Both JPAC and JPAC/TiO_2 adsorbents were characterized by the point of zero charges, Fourier transform of infrared spectroscopy, X-ray diffraction spectroscopy, Brunauer-Emmett-Teller analysis, and scanning electron microscopy with energy-dispersive X-ray analysis. The adsorption capacity of Reactive Red 194 (Red 2BN) dye on jackfruit peel activated carbon (JPAC) is 32.271 mg/g, and JPAC/TiO_2 is 34.900 mg/g was observed under optimum conditions. Desorption efficiency of JPAC/TiO_2 (≥93.4%) is slightly higher compared to JPAC (≥89.2%). Tannery effluents of various parameters were analyzed, and their chemical oxygen demand (COD) values trim down within the permissible limits of JPAC (97%) and JPAC/TiO_2 (98%). Experimental data were studied using both two-parameter and three-parameter models of adsorption isotherm, namely, the Langmuir, Freundlich, Temkin, Dubinin-Radushkevich, Redlich-Peterson, Sips, Toth, and Khan. In which the Langmuir isotherm ($R2 = 0.9824$) best described the experimental data with an optimum monolayer capacity for adsorption capacity of 49.7 mg/g at 323 K on Red 2BN molecules. A proposed scheme of Red 2BN molecules on the active sites of adsorbents was illustrated. Regeneration of spent carbons was studied through different cycles of the run.

1. Introduction

Synthetic dyes are used in textile and leather industries predominantly for contemporary dyeing and machinery deeds which in turn produce millions of tons of effluent, polluting the water resources. These coloring effluents are recalcitrant and also affect the microbial population by means of interrupting its oxidizing nature which will create esthetical impacts to the aquatic environment [1, 2]. The presence of dyes even in very small amounts in the water system is undesirable since dyes have been reported to be mutagenic and carcinogenic especially for human [1, 3, 4] . So, these effluents need some efficient treatment to meet the stringent limits as prescribed by Pollution Control Board (PCB) before discharging to the water resources, such as the Fenton process, sonochemical, Fenton hybrid biological treatment, biodegradation, photo-Fenton process, electrochemical, and electrochemical combined treatment [1, 2, 5]. However, certain limitations exist in the above treatment methods such as incomplete decolorization due to higher molecular weight, high production cost, and the large volume of sludge removal. Unflinchingly, the production of high-grade influent utilizing adsorption methods was found to be economically appealing under certain optimal conditions and trends of adsorption techniques were practiced due to their harmlessness to the ambiance, trouble-free operation, and

comparatively bulk effectiveness [2, 6]. Adsorption using activated carbon promises better adsorption of exceedingly high surface area and micropore volume, valuable assets for refinement, segregation, and remedial actions of organic compounds present in coloring agents, noteworthy sorption affinity, prompt adsorption kinetics, and virtually ease of regeneration. Essentially organic materials rich in carbon such as coal, lignite, and wood were preferably chosen as a precursor to scale up the production of activated carbon for commercial purposes was cost-effective. To overcome the situation, an assortment of carbonaceous biomass was chosen as precursor based on the availability, purity, denial of economic value, and probably the product manufacturing process and their application are imperative [7, 8]. Several pieces of research are carried using waste agricultural biomass such as coconut shell, grain sorghum, coffee bean husks, rubberwood sawdust, chestnut wood, and fruit stones and were found to be better adsorbents by the soaring nature of high carbon and low ash contents. [9–11]

Indian production rate of jackfruit (*Artocarpus heterophylls*) comprises to top ten states in which it varies from 291.59 to 49.73 tonnes in the year of 2015-2016 (NHB-HS Code 1047). By considering its wide variety of applications, a significant amount of jackfruit peel (JP) was discarded as waste which constitutes 59% of ripe fruit [12]. Few works have been carried out on JP activation using sulphuric acid for the removal of heavy metals [12, 13]. In this work, phosphoric acid acts as an activating agent for preparing carbon from the precursor of JP has been reported.

In addition to that, so many recent works focus on the preparation and modification of titanium dioxide (TiO_2) into ZrO_2/TiO_2, SiO_2/TiO_2, TiO_2-coated polystyrene spheres, TiO_2-and mounted exfoliated graphite, and composites of TiO_2/carbon were conveyed [14, 15]. Further, it confirms the coating of titania to the carbon surface enhances the breakdown of organic compounds in the photocatalytic process [14]. To be readily performed in the sorption process, TiO_2 materials must have a big size of particles and a high hardness. Recent research has revealed that the exposed crystalline faces of TiO_2 have a significant role in its adsorption efficiency. It is a never-ending quest to create TiO_2-based materials with good adsorption properties [16]. However, the use of these TiO_2 powders has some problems such as being nonviable for continuous operation because of the formation of particulate suspensions, and segregation of adsorbents from the reaction media leads to the consideration of supportive TiO_2 matrix as adsorbents. Indeed, promising results have been reported on AC and AC/TiO_2 from commercially available carbon but not with economically fewer value materials [17]. Moreover, the coating of TiO_2 particles onto the surface of AC was more uniform and proper by the sol-gel method [17]. Adsorbate is an azo dye of Reactive Red 194 that carries two different reactive groups of monochlorotriazine, and vinyl sulfone needs to be effectively adsorbed. These compounds come under "Category 2" carcinogen which is still in use as unnoticeable that handpicked three different pathways: ingestion, inhalation, and dermal absorption to cause neurosensory damage, metabolic stress, growth reduction, liver, and bladder cancer. To save endangered lives and to cure the issues by a minimal level through a large-scale manner were the targets in this work. By considering all the above statements, we made an attempt on selecting a designated substrate material as a precursor for the preparation of novel adsorbents for treating the adsorbate of higher molecular weight azo (Red 2BN) dye. The focus of this work concentrates on (i) checking whether a breakdown of organic molecules occurred under ambient conditions of prepared TiO_2 embedded on JPAC and (ii) reaching a novel adsorbent that is suitable for synthetic and real-time tannery effluent. (iii) Additionally, adsorbent should be easily recoverable with good regeneration capacity. (iv) Explore enhanced pores from less biomass material and reach neutral adsorbent which suits more specifically for both the charges of dyes (anion and cation).

To be specific about this research, $JPAC/TiO_2$ adsorbent was synthesized and employed to remove dye from tannery effluent wastewater of larger molecular structure. TiO_2 was chosen for various purposes, including its high mechanical strength and surface area, and it has been employed as a photocatalytic activity for degradation of organic pollutants. However, TiO_2 powder is easy to agglomerate, has poor adsorption capacity, and is difficult to separate and recycle from the solution, which are some of the downsides of using TiO_2 in advanced oxidation processes. For instance, many papers have suggested either adsorption or photocatalysis or by both through different combination of methods such as dip-hydrothermal using peroxotitanate as the TiO_2 precursor for degradation of methyl orange, sol-gel method for the degradation of methylene blue, impregnation and physicochemical pyrolysis, photocatalytic decomposition of an azo dye pollutant, and microwave-induced photocatalytic technology using TiO_2/AC composites [18–21]. For the purpose of overcoming, the drawback as well the activated carbon acts as a substrate for making a composite of adsorbents from a less value product to work with large scale and reproducibility. When compared to pure TiO_2, all types of TiO_2/AC composites have been found to have higher photocatalytic activity and increased removal efficiency in dye-containing wastewater treatment processes. However, because of the variability in the preparation and treatment methods, one of the main impediments to resumed large implementation of TiO_2/AC composites in wastewater treatment is the lack of reproducibility. As a result, a simple and inexpensive approach for preparing TiO_2/AC composites is required. However, to the best of our knowledge, many studies have focused on photocatalytic activity, degradation mechanism and kinetics, synergistic effects, and the role of the chemical and textural properties of AC in photocatalytic degradation of organic contaminants in wastewater, but there is little information on the effect of the smaller amount of loading cycle on the structural properties of the final TiO_2/AC composite without regard to photocatalytic activity as well for large-scale production from low-cost adsorbents was not focused.

Moreover, the combination of these adsorbents possesses a complete process and has an enhanced adsorption capacity by maintaining good stability all over the batch mode of the adsorption process. And a complete deletion

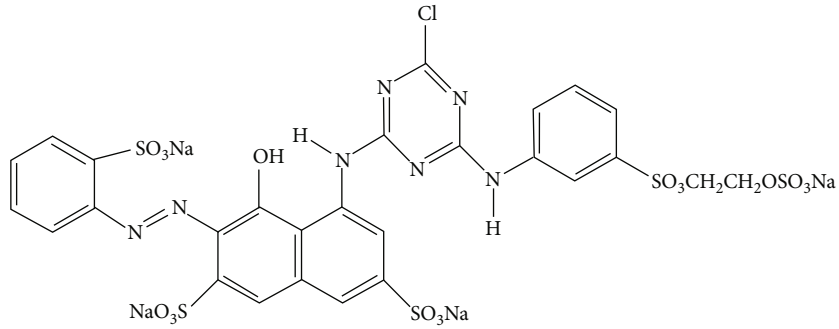

Figure 1: Structure of reactive Red 194.

of "Category 2" pollutants should be compulsory for the survival of natural habitats without collapsing the ecosystem through sustainable cheaper adsorbents. So that the research proposes a novel technique using JP to adsorb Red 2BN molecules which does not degrade under natural conditions.

2. Materials and Methods

JP was selected as a precursor for the preparation of activated carbon which was collected from the local shops in and around Neyveli, Tamilnadu. The adsorbate used in the current study was Red 2BN ($\lambda_{max} = 533nm$, 984.21 g/mol, $C_{27}H_{18}ClNa_4O_{16}S_5$) supplied from CLRI division, Chennai. Reactive Red 194 (RR194) is an azo dye named as Red 2BN with a purity of 75% ± 5 (CAS No. 23354-52-1) purchased by colourtex dyestuff company, Surat, Gujarat (India), and it is a complex aromatic structure consisting of functional groups such as chlorine, sulfonic groups, methyl, and amino groups, and its structure is given in Figure 1. This dye is widely used in leather industries, and both the raw effluent and the RR194 synthetic dye were also collected from the leather and tannery division of CLRI Chennai, Tamilnadu. The other materials used such as phosphoric acid (88 wt%) and sulphuric acid (98 wt%) were purchased from MERCK Private Ltd. Acetic acid (99%: extra pure) and sodium hydroxide (97% (CP)) were purchased from Ranbaxy Private Ltd. Potassium hydroxide (reagent grade, 90%,flakes), diethanolamine (ACS reagent, ≥99.0%), and ethanol (99%: extra pure) were purchased from SISCO Research Laboratory Private Ltd. Tetrabutylorthotitanate (reagent grade, 97%) was purchased from Alfa Aesar company. Methylene blue dye (70% ± 5), methyl violet, potassium iodate (≥98%), and potassium iodide (≥99.0%) were from Sigma Aldrich through SRL chem Private Ltd. Iodine (ACS reagent, ≥99.8%, solid) was purchased from Rankem, India. For real effluent, the following chemicals potassium dichromate (≥99.5%, ACS, Reag), silver sulphate (ACS reagent, 99%), mercury sulphate (ACS reagent, for preparation of solution for COD determination according to DIN 38409, part 41, ≥99%), ferrous ammonium sulphate (ACS reagent, 99%), ferroin indicator, organic free distilled water, calcium chloride (anhydrous, powder, ≥97%), magnesium sulphate (*ReagentPlus*, ≥99.5%), ferric chloride (reagent grade, 97%), dipotassium hydrogen phosphate (reagent grade, ≥98.0%), potassium dihydrogen phosphate (ACS reagent, ≥99.0%), disodium dihydrogen phosphate (anhydrous, 98-100.5%), ammonium chloride (ACS reagent, ≥99.5%), manganous sulphate (*ReagentPlus*, ≥99%), potassium hydroxide (reagent grade, 90%, flakes), sodium azide (*ReagentPlus*, ≥99.5%), and sodium thiosulphate (*ReagentPlus*, 99%) were required for COD and BOD analysis. All the reagents used for the analysis are of analytical grade with extra pure chemicals, and double-distilled water was used for preparing the adsorbate solutions. The working solutions were prepared as per the prescribed concentration by successive dilutions. The stock solution of 1000 mg/L was procured by dissolving a specified amount of Red 2BN in ACS reagent, 99% double-distilled water.

2.1. Preparation of Activated Carbon from Jackfruit. The outer pericarp of jackfruit peel (JP) containing a lot of flexible fibers was removed manually, and they were cut into small pieces. Surface-adhered particles and soluble components were removed from the peel by washing with warm water and taken the outer crust as major source for preparing the adsorbents. This was repeatedly continued until the water was colorless. Then, the material was dried in sunlight and oven-dried at 110°C till it reaches constant weight. The uniform dried slices were taken for soaking with the chemical activating agent by means impregnating the JP in phosphoric acid in the ratio of 1 : 1 (weight of activating agent/weight of raw material). The resulting slurry was then kept cooling for 24 h. After 24 h, the diluted form of acid was decanted and then the slurry was taken in sealed ceramic container inside the muffle furnace with the absence of air. The slurry gets carbonized at an activation temperature of 400°C with the heating rate of 5°rise/min of activating time 120 minutes. Then, the obtained product was resembles like flakes of AC was cooled and then repeatedly washed manually with water for removing the ions adhered on the surface. Then, with warm distilled water, the AC was shaken well in an orbital shaker until the pH of the solution was close to the initial pH of rinsing water. Finally, the activated carbon was dried in an oven at 110°C for 24 h. The dried slices were ground and sieved to obtain a particle size range of 0.063 mm. The selected size of the prepared activated carbon was taken as 240 mesh size (0.063 mm) throughout the study. [22, 23]. The same procedure was followed for preparing activated carbon using various activating agents such as sulphuric acid, acetic acid, sodium hydroxide, and potassium

hydroxide [8]. Further work was carried out using the best activating agent identified in the study. Activated carbon prepared from JP was characterized by proximate analysis using standard procedure was clearly discussed in supplementary section 1.

2.2. Preparation of TiO_2/AC Composite. JPAC used in the present study was prepared by chemical activation with a size of about 0.063 mm. Precursor solutions for JPAC/TiO_2 were prepared by the sol-gel method. Tetrabutylorthotitanate (8.51 mL) and diethanolamine (2.6 mL) were dissolved together in ethanol (64.82 mL), and the solution was stirred vigorously for 2 h followed by the addition of a mixture of distilled water (0.9 mL) and ethanol (10 mL) on stirring. The resulted alkoxide solution was left for hydrolysis reaction to result in TiO_2 gel. The 10 g JPAC was used as a support and immersed into the TiO_2 sol under ultrasonic assistance. After the sol-coated JPAC formed a gel, the TiO_2 gel-coated AC was dried at 130°C for 2 h in a hot air oven, and then, the calcination at a temperature of 500°C; finally, the sample was kept at this temperature for 2 h [14, 15].

2.3. Point of Zero Charge Measurement of Adsorbents (pH_{pzc}). The zero-surface charge characteristic of the adsorbents was determined using the standard method [24]. The experiment was conducted in a series of 250 mL of erlenmeyer flasks. NaCl solution of 0.01 M was prepared. The prepared NaCl solution was taken in each flask of 50 mL in which the pH values of the solution were adjusted between 2 and 12 by adding both 0.1 M HCl and 0.1 M NaOH. To that, 0.15 g of activated carbon and JPAC/TiO_2 was added. The suspensions were then sealed and shaken for 48 h at 180 rpm. The final pH values of the supernatant liquid were noted. The difference between the initial pH (pH_0) and final pH (pH_f) values ($\Delta pH = pH_0 - pHf$) was plotted against the pH_0. The intersection point of the obtained curve with abscissa, at which pH is zero, gives the pH_{pzc}.

2.4. Analytical Instrumentation. Solution concentration was analyzed by UV–visible spectrophotometer (SL159-Elico). The chemical structure and surface morphology of the adsorbents were studied by FTIR (Shimadzu, Happ-Genzel, EDX-8000) and SEM/EDAX (Ametek instruments, Chennai). Similarly, the particle nature, pore size distribution, and surface area of the adsorbents were depicted using BET (Belsorp HP, Microtrac, Belcorp) analysis.

2.5. Adsorption Studies. Equilibrium adsorption studies were conducted by contacting 50 mL of Red 2BN dye solution of different initial concentrations with 0.5 g of adsorbent in a glass erlenmeyer conical flask. The samples were shaken until equilibrium is reached. Then, solutions were centrifuged, and supernatant solutions were analyzed. The equilibrium adsorption capacity, q_e (mg/g), at different dye concentrations, was determined by the following equation:

$$q_e = \frac{(C_i - C_e)V}{m}, \tag{1}$$

where C_i (mg/L) is the initial concentration, C_e (mg/L) is the equilibrium concentration in the liquid phase, V is the volume of liquid phase (L), and m is the mass of the adsorbent (g). Study the nature of adsorption, effects of contact time, concentration, carbon loading, pH, and temperature.

2.6. Isotherm Studies. Considering a framework of abundant records on adsorption isotherm that tends to deliver the difference in their nature of sorption on the surface affinity with the two-parameter and three-parameter models of JPAC and JPAC/TiO_2 was discussed clearly in supplementary section 2 and 3 [1, 25]. Also, the clear view and importance of error functions are mentioned in supplementary section 4.

2.7. Adsorption Mechanism and Thermodynamic Studies. Thermodynamic parameters of adsorption explain the nature of the process through Gibb's free energy (ΔG°), entropy (ΔS°), and enthalpy (ΔH°), and their equations are given below.

$$\begin{aligned} K_C &= \frac{C_{Ae}}{C_e}, \\ \Delta G^\circ &= -RT \ln K_C, \\ \log K_C &= \frac{\Delta S^\circ}{2.303R} - \frac{\Delta H^\circ}{2.303RT}, \end{aligned} \tag{2}$$

where C_{Ae} is the amount of Red 2BN molecules adsorbed onto the active sites of sorbent during adsorption (mg/g), C_e is the equilibrium concentration, R is gas constant (8.314 J/molK), T is the temperature (K), and K_C is the equilibrium constant.

2.7.1. Intraparticle Diffusion Model. To predict the rate-limiting step of adsorbate onto the surface of active sites was considered through the intraparticle diffusion model given in Equation (3), in which the weight uptake and time explain the relationship between the adsorbate and adsorbent majorly through three stages: film diffusion, surface diffusion, and pore diffusion [26, 27].

$$q_t = K_{id} t^{0.5} + C, \tag{3}$$

where K_{id} is the intraparticle diffusion rate constant (mg/g.min$^{-0.5}$) and c is the film thickness constant of adsorbate and adsorbent. And assuming carbon to be a sphere (r) that follows the Fick law of diffusion corroborates the weight acceptance and time is given as

$$F(t) = 6\left(\frac{D_t}{r^2}\right)\left\{\pi^{-1/2} + 2\sum_{n=1}^{\infty} ierfc\frac{nr}{\sqrt{Dt}}\right\} - 3\left(\frac{D_t}{r^2}\right), \tag{4}$$

where $F(t)$ is the fractional attainment of equilibrium at a time in which $F(t) = q_t/q_e$.

At smaller times, $D = D_1$ (Equation (4)) reduces to

$$\frac{q_t}{q_e} = 6\left(\frac{D_1}{\pi r^2}\right)^{1/2} t^{1/2}. \quad (5)$$

At moderate times,

$$F(t) = 1 - \frac{6}{\pi^2}\sum_{n=1}^{\infty}\frac{1}{n^2}\exp\left[-n^2 B_t\right], \quad (6)$$

where D_e is the effective diffusion coefficient (m^2s^{-1}) $B = \pi^2 D_e/r^2$.

At longer times,

$$\ln\left(1 - \frac{q_t}{q_e}\right) = \ln\frac{6}{\pi^2} + \left(\frac{-D_2\pi^2}{r^2}\right)t. \quad (7)$$

2.8. Kinetic Studies. Adsorption kinetic study describes the rate of adsorbate molecule uptake in the active sites which in turn tells the residing time in the adsorption process. To understand the behavior of Red 2BN molecules on the surface was judged by rate equation such as pseudofirst-order (Lagergren 1898), pseudosecond-order [28], and the Elovich model defines undoubtedly Equation (8).

$$\begin{aligned} q_t &= q_e[1 - \exp(K_1 t)], \\ q_t &= \frac{k_2 q_e^2 t}{1 + k_2 q_e t}, \\ q_t &= \frac{1}{\beta\ln(a\beta)} + \frac{1}{\beta\ln(t)}, \end{aligned} \quad (8)$$

where k_1 and k_2 are pseudofirst constant and pseudosecond order constant and a and β are Elovich constants.

2.9. Characterization Methods on Real Effluents. The effluent samples were collected in a sterilized container. Containers were thoroughly rinsed with samples at the collecting station, then filled with samples, corked tightly, and sent to the laboratory for treatment and analysis. The methods of analysis are as follows: 3025 (parts 16 and 17) (part 44) (part 58)—APHA standard methods for the assessment of water and wastewater-20th edition method 2540C and 2540D for dissolved/suspended solids, method 5210B for BOD analysis, and method 5220C for COD analysis [29]. The COD digester (CR25, Spectral lab instruments-India), BOD (Tanco BOA-10 (capacity 282 Ltr)), and Hach 145701 Hardness Test Kit, Model HA-4P MG-L were used.

2.9.1. Experimental Procedure for COD and BOD. Batch adsorption equilibrium experiments were carried out by contacting a specified amount of adsorbent with 50 ml wastewater sample, of a known initial COD concentration, in a sealed glass bottle. The COD uptake was determined as a function of time, using 0.5 g/L JPAC and JPAC/TiO_2, contacted with tannery wastewater samples obtained from a leather division of CLRI, Chennai. Wastewater samples of three replicate initial concentrations, namely, 4000 (±0.5) mg/L, were tested. The bottle was kept on a shaker for 4 h to reach equilibrium at an optimum temperature. At regular intervals, samples were withdrawn in COD vials with/without wastewater kept in COD digester. After cooling to room temperature, the samples were titrated against ferrous ammonium sulphate with ferroin as indicator. In addition, the experiment was carried at different values of temperature and pH to determine their effects with that of optimum conditions. Similarly, the BOD concentration of wastewater sample was analyzed by means of BOD incubator. The samples were kept in BOD incubator for 5 days at 20°C. The uptake, q_e, was then calculated from the difference between the initial and the final values of COD and BOD analysis during the sequence of run using Equation (1).

Table 1: Nature of biomass and their properties.

Properties	Raw	JPAC	JPAC/TiO_2
Extractives	14.73	-	-
Hemicellulose (%)	35.2	-	-
Cellulose (%)	39.4	-	-
Lignin (%)	7.2	-	-
Ash content (%)	4.31	6.24	-
Moisture content (%)	13.53	4.97	-
Fixed carbon (%)	33.02	86.21	-
Volatile matter (%)	49.14	2.58	-
Iodine number (mg/g)	177.27	510.83	734.45
Methylene blue number (mg/g)	20	103	145
Methyl violet number (mg/g)	24	182	159
Bulk density (g/mL)	0.48	0.69	0.74
Yield (%)	-	68.4	
Activation temperature (°C)	400		
Chemical activating agent	H_3PO_4, H_2SO_4, CH_3COOH, NaOH, KOH		

3. Results and Discussion

3.1. Proximate Analysis of Adsorbents. Initially, the extractives, cellulose, hemicellulose, and lignin content were examined on a dry basis by tappi protocol method of T 212 om-02 to verify the nature of the biomass [30]. Lignocellulosic material reboots the presence of carbon matrix which in turn insists the study of the adsorbents through iodine number, methylene blue number, methyl violet number, and point of zero charge. The preliminary properties of selected biomass are depicted in Table 1.

3.1.1. Point of Zero Charge of Adsorbents. The pH_{pzc} of an adsorbent is an essential characteristic bound that determines the pH at which the adsorbent surface has net electrical neutrality. From Figure 2. the point of zero charge for activated carbon and JPAC/TiO_2 composite is found to be 5.4 and 7.4, respectively. The TiO_2 impregnation of the carbon surface has changed the pH of the modified carbon sample which indicates that the surface of JPAC/TiO_2 is almost neutral ($pH_{zpc} = 7.4$) whereas the surface of AC is an acidic

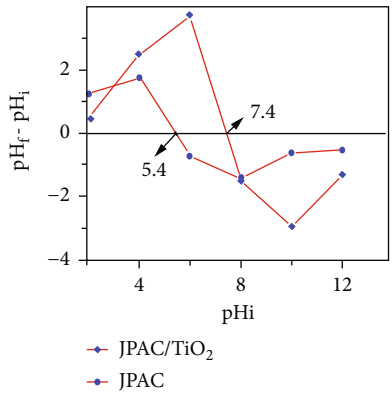

Figure 2: Point of zero charge plot of adsorbents by drift method.

one ($pH_{zpc} = 5.4$). In accordance with the enhancement of active sites as well as the adsorbent becomes more susceptible to both anionic and cationic dyes, an attempt was made to immobilize the TiO_2 particles on JPAC using the sol-gel method renders a change in this point of zero charge value from 5.4 to 7.4 may be due to the result of surface oxidation thus contributes an increased hydroxyl competition tends to be neutral [24]. Further, the concentration of TiO_2 particles gets increased leading to a change in the charge density higher to 7.8 and so on. To proceed further, an increment in TiO_2 amount gets stopped to fix the neutral adsorbent. The pH_{zpc} value renders both adsorbents to be more suitable in the removal of anionic dyes such as Red 2BN from contaminated water systems.

3.1.2. Thermogravimetric Analysis of Adsorbents. To examine the decomposition characteristics of JP thermogravimetric analysis was performed and shown in Figure 3(a). Initial weight loss before 245.53°C could be attributed to the removal of moisture and other volatile materials. A sharp dip in percentage weight loss of 66% by a step transition is observed in the range between 245.53°C and 356.37°C which is attributed to the decomposition of hemicellulose, cellulose, and lignin present in JP. It is illustrated in Figure 3 in which the weight loss of the material is the function of the decomposition temperature, and it depends on lignocellulosic material undergone dehydration, depolymerization, and constituent biopolymer relocation [31, 32]. The DSC (differential scanning calorimetry) exothermic decomposition occurs at 324.72°C; hence, temperature above this value is preferable for activation. Similarly, to examine the decomposition characteristics of JPAC/TiO_2 voices, the higher solid residue confirms the nature of withstanding capacity at high temperature shown in figure 3(b). The temperature ranges 50-950°C at 20°C/min of heating ramp by purging nitrogen at the rate of 150 mL/min with platinum as reference. Generally, the thermal analysis of organic and inorganic compound results the formation of residual carbon on heating is carried out at nitrogen atmosphere, and this residual material percentage is a function of maximum heating temperature. The incomplete decomposition of biosorbents containing the constituents of carbon, oxygen, hydrogen, and inorganic compounds could represent the residual matter. So the high percentage of (>50%) residual weight implies the carbonaceous materials and inorganic metal oxides.

3.1.3. FTIR Analysis. The functional groups of JPAC and JPAC/TiO_2 spectrum are illustrated in Figure 4 using FTIR. JPAC can be interpreted as a broad adsorption band around 3400-2400 cm^{-1}, in which it is assigned to the stretching vibration of O-H bonds of surface adsorbed water molecules [33]. The adsorption band around 2970-2250 cm^{-1} shows a very weak peak of stretching vibration C-H bonds in the methyl group. A sharp peak around 1650-1590 was attributed to the bending vibration of the C=C aromatic ring which was enhanced by polar functional groups. There was a band around 1300-1000 cm^{-1}, and this shows the peak at 1220-1180 cm^{-1} may be ascribed to the stretching mode of hydrogen-bonded P=O, O-C stretching vibrations in P-O-C linkage, and P=OOH; the shoulder at 1080-1070 cm^{-1} can be ascribed to ionized linkage P+ -O- in acid phosphate esters and to symmetrical vibration in a chain of P-O-P [16, 34, 35]. In the case of JPAC/TiO_2, a broad absorption band around 3400-2400 cm^{-1} was assigned to be stretching vibration of O-H groups in which the carbon-loaded TiO_2 surface is rich in hydroxyl groups. A fragile peak of 2362.513 cm^{-1} bands is attributed to be bending of C-H bonds, whereas 1613.515 cm^{-1} band originates from the stretching vibration of C=C bonds of the JPAC framework. Once the TiO_2 species were loaded, the intensities of these bands increased. These increased functional groups are distributed on the JPAC surface which is advantageous for the adsorption and removal of organics from aqueous solutions. The broad absorption band in the range of 400 to 800 cm^{-1} is attributed to the Ti-O and Ti-O-Ti vibration [36]. Therefore, the range of 667.019 cm^{-1} absorption band suggests that TiO_2 is bonded to the AC surface. However, with the addition of AC, a new peak was included at the absorption band at about 1076 cm^{-1} may be ascribed to Ti–O–C, indicating a slight connection effect between bulk AC and Ti–O bonds. From the functional group analysis, the prepared JP activated with H_3PO_4 is in acidic surface groups which further confirms the pH_{pzc} of JPAC was 5.4 but in the case of JPAC/TiO_2, the surface becomes almost neutral. After adsorption from Figure 4, the FTIR spectrum tends to shift the peak ranging from 1237.152 cm^{-1} to 1400.344 cm^{-1}, and 1192.993 cm^{-1} to 1531.535 cm^{-1} correspond to the reduction of carbonyl and carboxyl group by means of interaction of Red 2BN dye molecules with carboxylates onto the surface of JPAC and JPAC/TiO_2. Also, there is a shift in the range from 2389.844 cm^{-1} to 3938.765 cm^{-1} for JPAC, and 2358.788 cm^{-1} to 3856.733 cm^{-1} for JPAC/TiO_2 indicate the existence of amino and hydroxyl groups. Besides, there is peak shift from 3206.711 cm^{-1} to 3912.681 cm^{-1} for JPAC, and 3428.254 to 3801.761 cm^{-1} embody the presence of hydroxyl radicals. In addition, there is a peak shift from 415.667 cm^{-1} to 756.452 cm^{-1}, and 433.027 cm^{-1} to 752.251 cm^{-1} correspond to halogenated alkane, C-H aromatic, and C-C functional groups. The range of 756.452 cm^{-1} to 1099.444 cm^{-1} shows the presence of C-H aromatic meta and parasubstituted benzene functional

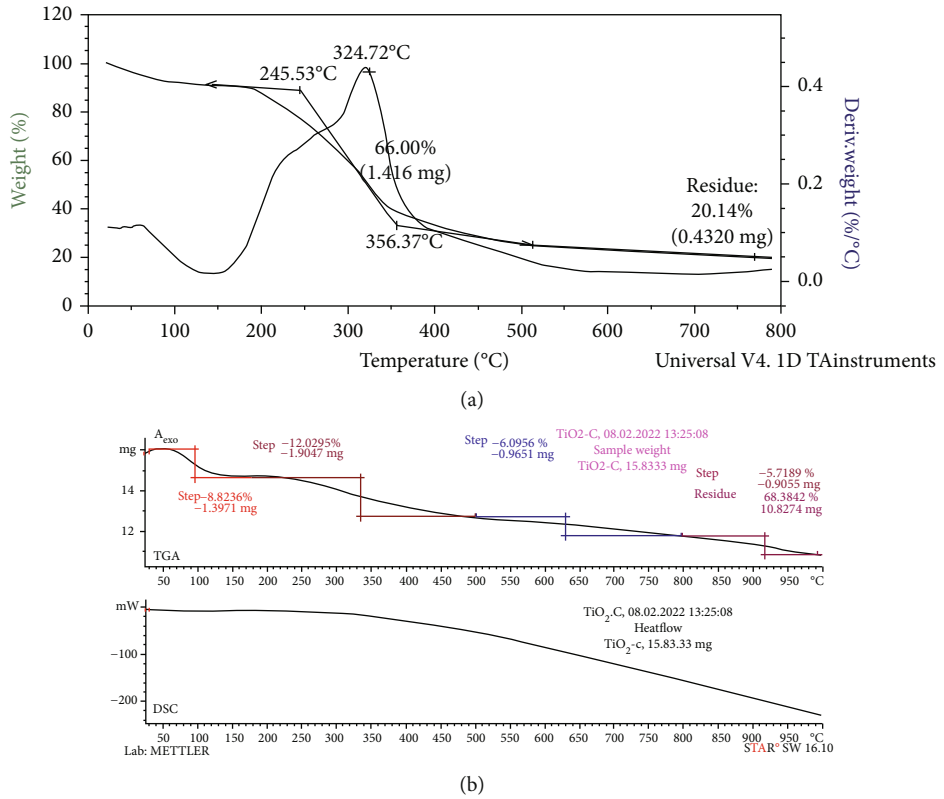

Figure 3: Thermogravimetric analysis of jackfruit peel biomass.

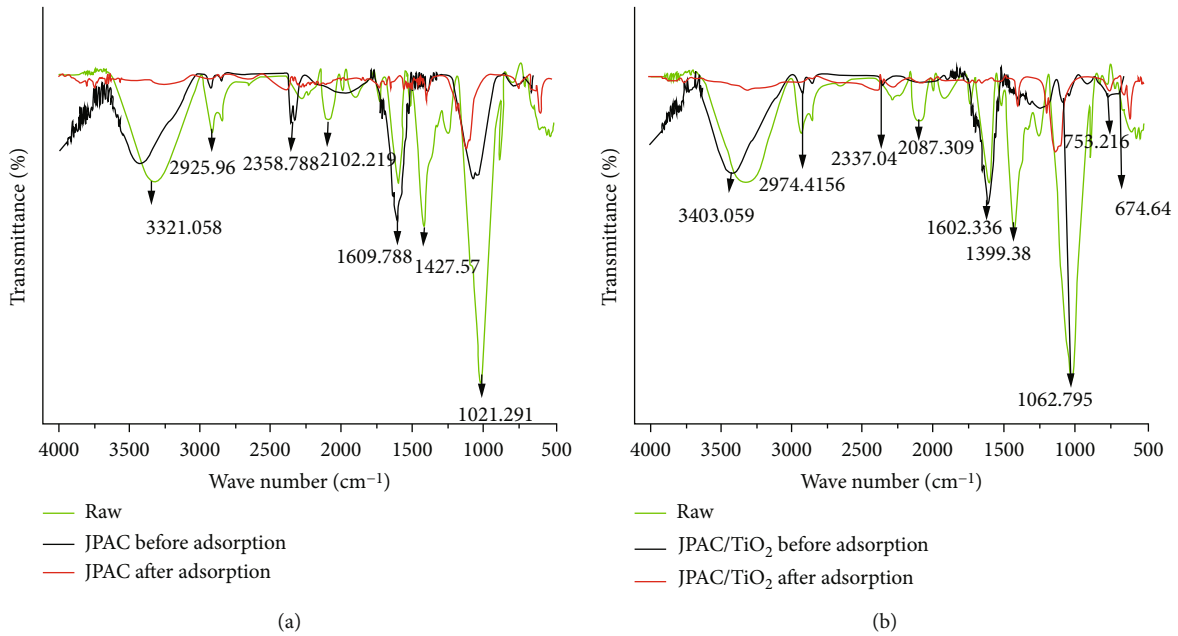

Figure 4: FTIR analysis of (a) JPAC and (b) JPAC/TiO_2.

groups of finger print region [37]. All the peaks are drawn by baseline corrections for depicting the spectral peaks.

3.1.4. BET Analysis. The nitrogen adsorption-desorption isotherms of raw, JPAC, and JPAC/TiO_2 were measured using a BET analyzer. A density functional theory (DFT) model was used to predict the pore size distribution. Prior to the nitrogen adsorption examination, all samples were degassed under vacuum for 12 hours at 200°C, in which the raw and activated carbon incorporated TiO_2 adsorbents indicate the

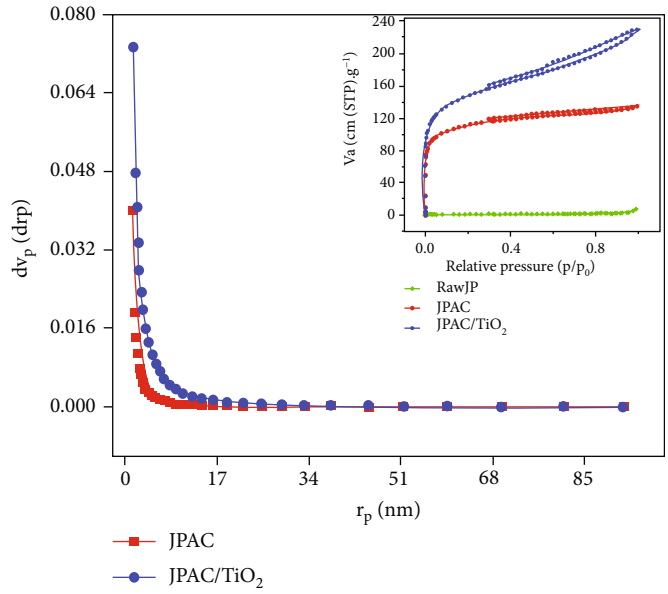

Figure 5: N_2 adsorption-desorption isotherms of JPAC and JPAC/TiO_2 by BET analysis.

Table 2: Physical properties of activated carbon from jackfruit peel using BET analysis.

BET properties	Adsorbents		
	Raw Jackfruit	JPAC	JPAC/TiO_2
BET surface area (a_s) (m^2/g)	2.9931	389.3402	513.0401
Monolayer volume (cm^3/g)	0.6877	89.4530	117.8703
Total pore volume (cm^3/g)	0.0112	0.2093	0.3556
Mean pore diameter (nm)	14.9680	2.1505	2.7725

typical trend of type II adsorption isotherm but in case of JPAC, resembles like type IV fashion were represented in the plot as shown in Figure 5.

The adsorbents having a hysteresis loop commonly associated with microporous and mesoporous attributes are also commented in paper [38]. Moreover, the properties of adsorbents were further corroborated by the values obtained in BET analysis depicts the nature of biomass gets enhanced from lower to higher surface area as shown in Table 2. The surface area of JPAC was increased compared with raw JP because of the enhancement of pores due to activation time and temperature. Essentially, JPAC/TiO_2 composites are microporous materials. Desorption hysteresis loops are also visible in the isotherms of JPAC and JPAC/TiO_2 composites at a relative pressure of roughly 0.5, implying the presence of some mesopores. The pores of JPAC and JPAC/TiO_2 composites are scattered in the range of 2.15–2.77 nm, and the mesopores are predominantly distributed between 2.2 nm and 5.0 nm, as shown by the curves of the DFT pore size distributions of JPAC and JPAC/TiO_2 composites (Figure 5). Furthermore, when compared to the original JPAC, the micropores of JPAC/TiO_2 composites steadily grow with increasing loading cycle, particularly for pore distributions in the 0.5–1 nm range in Table 2. The explanation for this can be linked to the fact that fewer loading cycles result in fixed TiO_2 particles, which do not appear to restrict micropores in the JPAC substrate. S_{BET} and V_t steadily increase with impregnation in JPAC/TiO_2 composites. The increment of V_t in JPAC/TiO_2 is mainly caused by the TiO_2 particles adhered on the AC surface and forms a small number of mesopores in the composite adsorbents to increase the pore volume. In addition, it is worthy of noting that S_{mic} and V_{mic} of composite decrease was informed in this paper [39] by loading TiO_2 higher. The results further confirm that micropores are not blocked or covered by the TiO_2 particles by lesser loading of TiO_2 particles.

3.1.5. SEM Analysis. The morphology of JP activated carbon (JPAC) and modified carbon JPAC/TiO_2 was ascertained by SEM/EDAX as shown in Figures 6(a) and 7(a). Figure 6(a) depicts the presence of holes like a honeycomb shape or in a view of a spherical rod which in turn confirms the platform for the sorption of Red 2BN molecules. Also, Figure 7(a) shows a tiny hole with an internal surface, and roughness on the surface sites with the adhered nature of TiO_2 particles was observed. Both the adsorbents were accredited to the enhanced surface area having voids of predominately wide mouth for the uptake of larger molecules. It further confirms by the EDAX chart of JPAC and JPAC/TiO_2 with carbon 79.75% and TiO_2 as 15.47%. In addition to that, the presence of pores was confirmed through BET analysis having a higher surface area for TiO_2-loaded JPAC. And after adsorption, the larger molecules get blocked or adhered on the active sites and the holes present on the surface void get closed was portrays in Figures 6(b) and 7(b).

3.2. Adsorption Studies. The activating agent plays a triggering role in preparing adsorbents with improved active sites which can be observed by impregnating biomass both by acids and bases. The percentage of adsorption is as follows: CH_3COOH: 59.42%, H_3PO_4: 93.71%, H_2SO_4: 69.73%, NaOH: 74.65%, KOH: 56.2%, and commercial activated

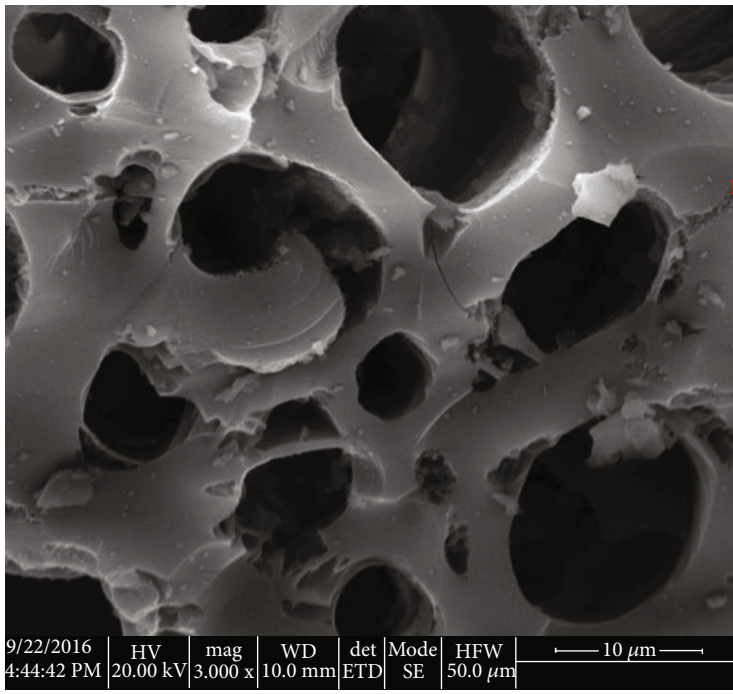

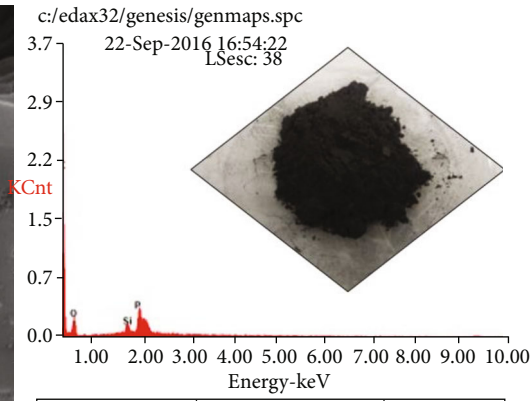

Element	Wt%	At%
CK	79.75	85.50
OK	15.49	12.47
SiK	01.17	00.54
PK	03.58	01.49
Matrix	Correction	ZAF

(a)

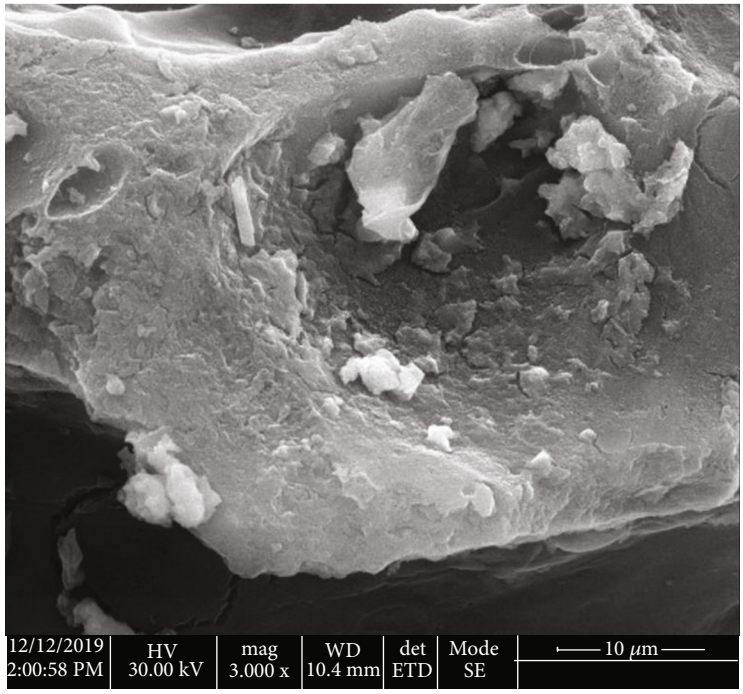

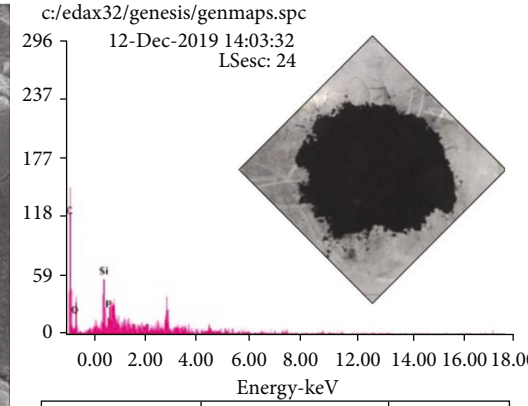

Element	Wt %	At %
CK	77.34	83.37
OK	17.93	14.52
SiK	03.13	01.44
PK	01.59	00.67
Matrix	Correction	ZAF

(b)

Figure 6: (a) SEM morphology and EDAX plot of JPAC before adsorption.

carbon: 66.3%. The results show that phosphoric acid has a high % of adsorption due to its high degree of microporosity and enhanced polar characteristics compared with other activated carbons [40–42]. Herewith, the further activation of biomass was focused on phosphoric acid.

3.2.1. Effect of Concentration and Contact Time. The effect of contact time on different concentrations of Red 2BN was observed for JPAC and JPAC/TiO_2. Both adsorbents show good performance of adsorption capacity which is shown in Figures 8(a) and 8(b). The adsorption process increases sharply at the initial rate, indicating the availability of readily manageable active sites. Gradually, the process gets slower once equilibrium is attainted. From the bulk solution, Red 2BN molecules tend to occupy the external surface of adsorbents, gradually when time proceeds the molecular uptake is

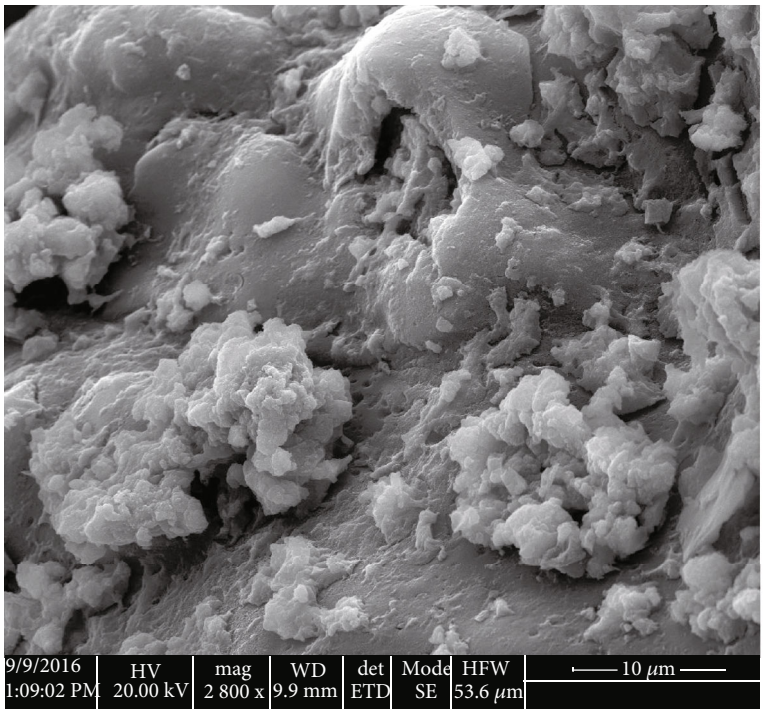

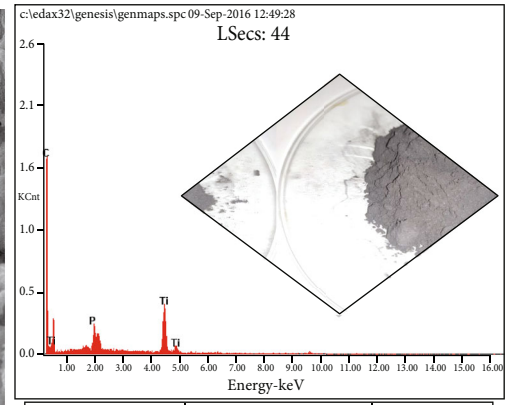

Element	Wt %	At %
CK	80.97	93.90
PK	03.56	01.60
TiK	15.47	04.50
Matrix	Correction	ZAF

(a)

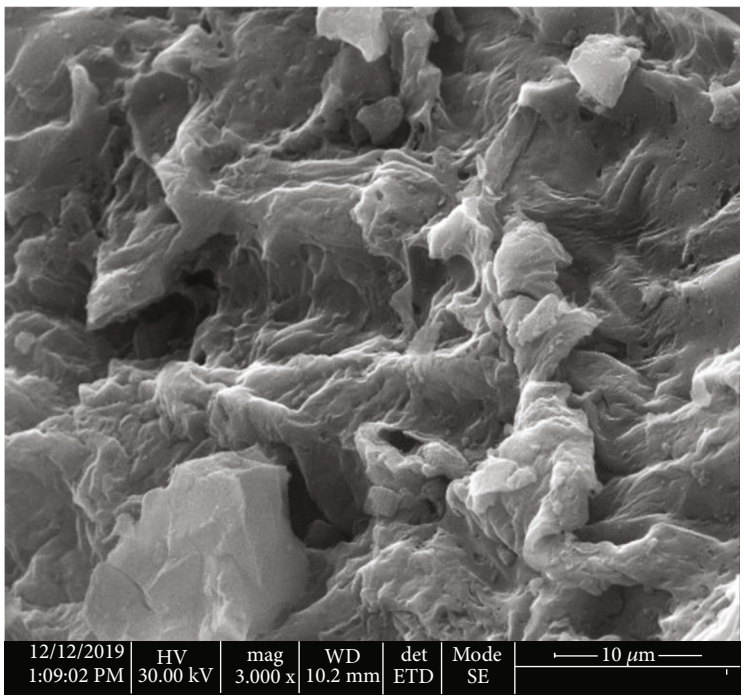

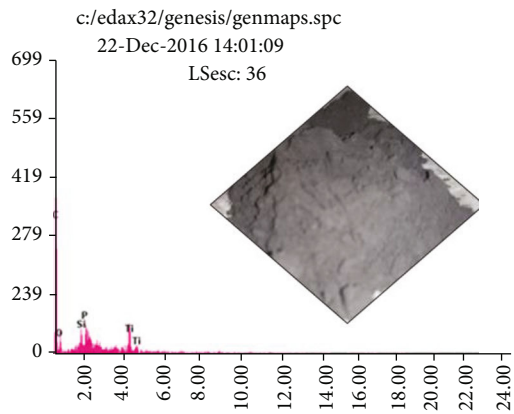

Element	Wt %	At %
CK	79.78	86.26
OK	14.48	11.76
SiK	01.20	00.55
PK	01.32	00.55
TiK	03.22	00.87
Matrix	Correction	ZAF

(b)

Figure 7: (a) SEM morphology and EDAX plot of JPAC/TiO_2 before adsorption.

controlled from the exterior to the interior sites of the adsorbent. The necessary time to attain equilibrium is about 4 h for both JPAC and JPAC/TiO_2 while titanium oxide incorporated activated carbon starts to rise faintly at higher concentrations. And that the change in the initial concentration of Red 2BN does not affect the attainment of equilibrium. Therefore, the effect of contact time on adsorbents increased with an increase in contact time in which the

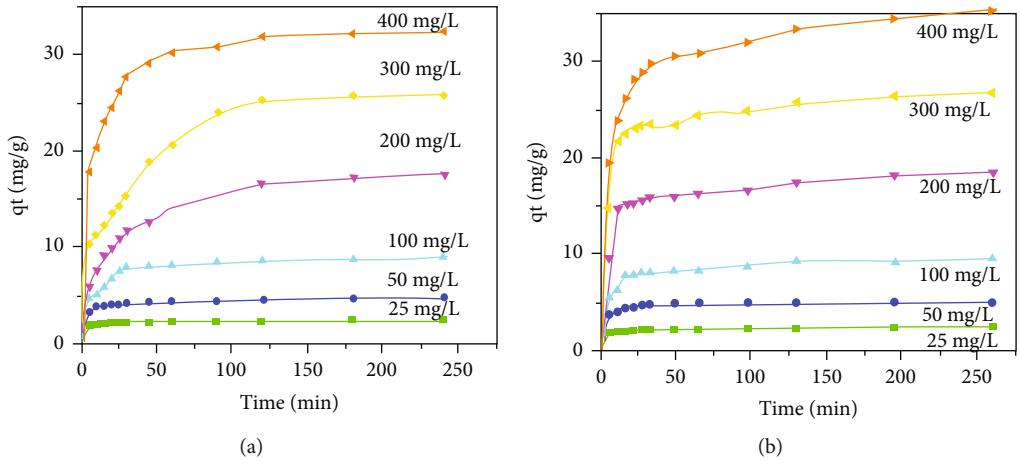

Figure 8: Effect of concentration and contact time of Red 2BN on (a) JPAC adsorption and (b) JPAC/TiO_2 adsorption (adsorbent dose = 0.5 g, pH = 6.5 (solution pH), and T = 303 K).

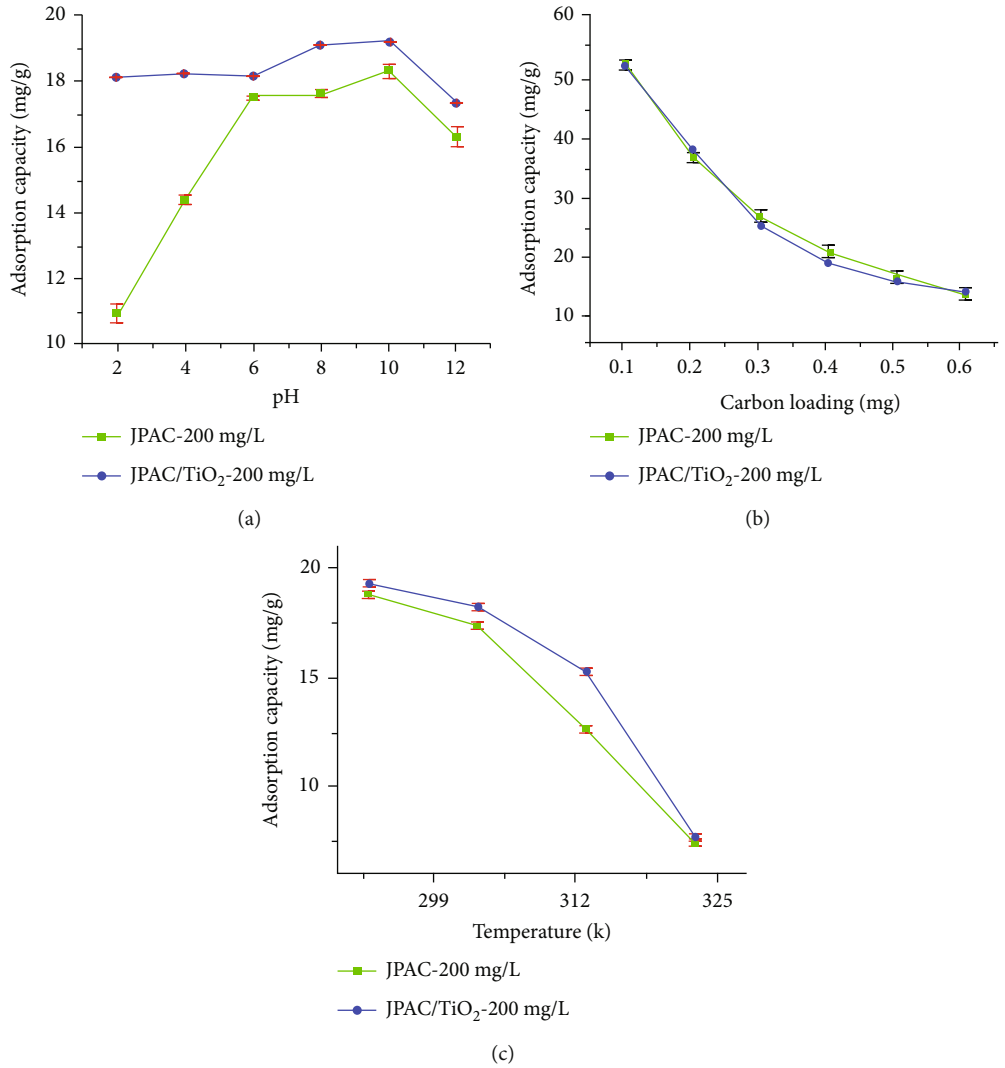

Figure 9: Effect of (a) pH, (b) carbon loading, and (c) temperature of Red 2BN dye on JPAC and JPAC/TiO_2 adsorption (adsorbent dose = 0.5 g, Ci = 200 mg/L, pH = 6.5 (solution pH), T = 303 K, and contact time = 4 h).

Table 3: Thermodynamic properties of JPAC and JPAC/TiO_2.

Adsorbents	Initial concentration (mg/L)	ΔH° (kJ/mol)	ΔS° (kJ/mol·K)	$\Delta G^\circ \times 10^4$ (kJ/mol)			
				293 K	303 K	313 K	323 K
JPAC	50	-88.1870	-0.2688	-2.410	-2.500	-2.580	-2.671
	100	-72.9390	-0.2226				
	200	-67.9840	-0.2074				
JPAC/TiO_2	50	-77.4110	-0.2340	-2.530	-2.620	-2.711	-2.790
	100	-76.2140	-0.2300				
	200	-73.4460	-0.2230				

Table 4: Kinetic constants of Red 2BN on JPAC and JPAC/TiO_2.

Adsorbent	C_i (mg/L)	q_e expt (mg/g)	Pseudofirst-order model			Pseudosecond-order model				Elovich model		
			q_e Calc (mg/g)	k_1 (min^{-1})	R^2	h (mg/g·min)	k_2 (g/mg·min)	q_e (mg/g)	R^2	α (mg/g·min)	β (g/mg)	R^2
JPAC	25	2.500	0.6226	0.0078	0.4083	0.2013	0.0822	2.4491	0.9959	7359.324	6.5090	0.9762
	50	4.686	0.9698	0.0143	0.6505	0.3201	0.06824	4.6904	0.9995	4813.15	3.1626	0.9159
	100	8.929	1.8432	0.0166	0.6813	0.3521	0.0393	8.9605	0.9998	18.329	0.8715	0.8639
	200	17.529	3.5969	0.0168	0.7268	0.3451	0.0196	17.605	0.9997	3.9086	0.3125	0.9902
	300	25.614	5.320	0.0192	0.7786	0.3608	0.0140	25.773	0.9998	5.0775	0.2063	0.9429
	400	32.271	8.3595	0.0200	0.8239	0.2899	0.0089	32.573	0.9998	99.0113	0.2545	0.9327
JPAC/TiO_2	25	2.860	0.8440	0.0157	0.7683	0.2263	0.0900	2.5144	0.9900	30765.31	7.1659	0.9617
	50	5.000	1.6060	0.0730	0.9218	0.3932	0.0775	5.0735	0.9998	151244.4	3.6959	0.8228
	100	9.532	2.0698	0.0149	0.9410	0.0728	0.0074	9.8425	0.9951	139.6931	1.0792	0.8782
	200	18.340	2.9561	0.0115	0.9419	0.0456	0.0024	19.0114	0.9886	497.9234	0.5976	0.7696
	300	26.540	3.4525	0.0114	0.9312	0.0468	0.0017	27.5480	0.9888	1414.596	0.4360	0.7486
	400	34.900	3.5604	0.0136	0.8952	0.0605	0.0017	35.5871	0.9923	264.3533	0.2731	0.9410

adsorption capacity of JPAC and JPAC/TiO_2 was maximum to the extent of 32.271 mg/g and 34.900 mg/g, respectively, for an initial concentration of 400 mg/L.

3.2.2. Effect of pH. pH is a crucial parameter in the adsorption process because it influences the degree of ionization of the adsorbate molecules, adsorbent surface charge density, and dissociation of available functional groups on adsorbent surface and structure [43, 44]. From Figure 9(a), the uptake of Red 2BN molecules from bulk solution by both JPAC and JPAC/TiO_2 has a positive effect on pH. The removal efficiency was increased from 56 to 81% and 91 to 96%, respectively, for JPAC and JPAC/TiO_2. These substantial increase and decrease in the uptake of Red 2BN molecules can be corroborated based on pH_{zpc}. As specified earlier, below pH_{zpc} surface of adsorbents is positively charged which in turn result shows a competition between the H^+ and dye cations to reach the active sites. Probably the surface is already surrounded by H^+ which in turn limits the interaction between the Red 2BN molecules to the active sites through repulsive forces. It leads to the contribution of fall in adsorption capacity at lower pH but an enhancement in the uptake of Red 2BN molecules at higher pH confirms the interaction of active sites. Similarly, TiO_2-loaded carbon behaves as an almost neutral adsorbent for a range of pH 2 to 10, and at pH 12, it tends to decrease the adsorption capacity may be due to the formation of hydroxide which tends to remark that $pH > pH_{zpc}$. To be more specific, it is evident that both electrostatic forces and cation exchange capacity of adsorbents were responsible for the prominent uptake of Red 2BN molecules.

3.2.3. Effect of Carbon Loading. The effect of carbon loading of both adsorbents was considered to predict the required amount of carbon in the adsorption process as shown in Figure 9(b). The graph tells the amount of uptake of Red 2BN molecules increases by increasing the amount of loading, and the adsorption capacity decreases depending upon the binding sites available on the surface in addition that the availability of exchange of sites gets more when the amount of carbon gets increased which means active sites remain unsaturated [42, 45].

3.2.4. Effect of Temperature. The temperature effects of the adsorption process tell the feasibility of the spontaneous progression. Here, reduction in adsorption capacity by increasing the temperature from 293 to 323 K is observed in Figure 9(c). This reduction on both adsorbents when increasing the temperature suggests that the process was exothermic. This is due to the fact adsorbed Red 2BN molecules have greater vibrational energies that tend to desorb from the active sites. Based on adsorption equilibrium data, thermodynamic parameters were predicted for JPAC and JPAC/TiO_2 as shown in Table 3. From Table 3, negative values of ΔG° for both adsorbents outline the feasibility of the impulsive process, and the system exhibits randomness.

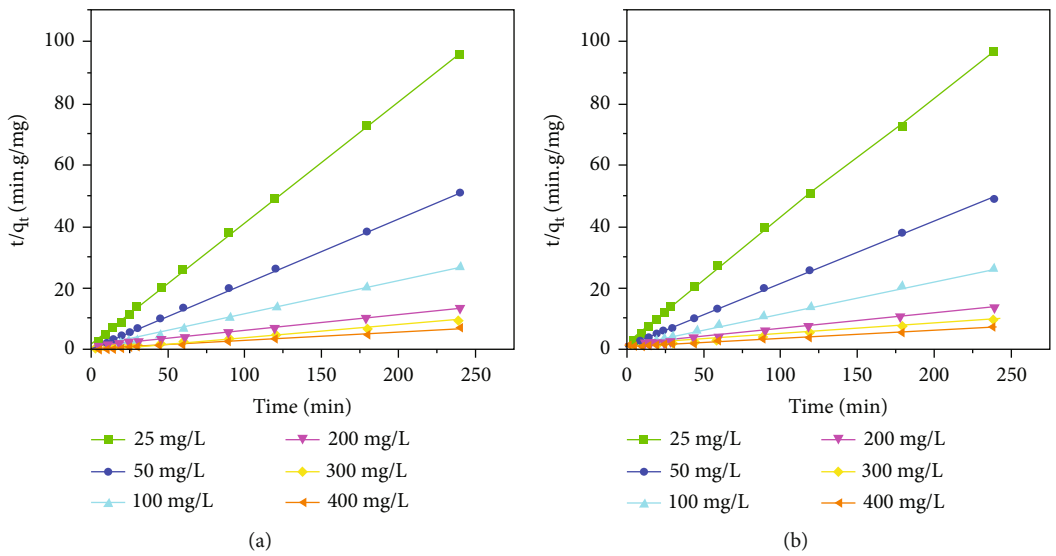

Figure 10: Plot of pseudosecond-order model for (a) JPAC adsorption and (b) JPAC/TiO_2 adsorption at different concentrations.

Table 5: Adsorption isotherm parameters of JPAC and JPAC/TiO_2.

Two-parameter isotherms	JPAC	JPAC/TiO_2	Three-parameter isotherms	JPAC	JPAC/TiO_2
Langmuir			Redlich-Peterson		
K_L (L/g)	0.0208	0.0335	K_R (L/g)	1.1246	1.4926
a_L (L/mg)	1.0940	1.7823	a_R $(L{\cdot}mg)^{1/B-1}$	0.9661	0.8362
R^2	0.9839	0.9948	B	0.0251	0.4425
SSE	9.2130	3.9120	R^2	0.97858	0.9330
RMSE	1.5180	15.6481	SSE	3.0691	10.9802
			RMSE	9.2072	32.9407
Freundlich			Sips		
K_F $(mg/g/(mg/L)^{(1/n)})$	2.5490	3.8226	K_s (L/g)	1.3820	4.4547
N	1.6915	1.7937	a_s (L/mg)	0.0226	0.3567
R^2	0.9819	0.9597	n	1.1000	1.1120
SSE	3.2425	8.23515	R^2	0.9876	0.9353
RMSE	12.96998	32.94059	SSE	2.9635	10.5992
			RMSE	8.8904	31.7975
Temkin			Toth		
A_T (L/mg)	0.3877	0.4719	q_T (mg/g)	32.7018	18.781
b_T (J/mol)	0.2862	0.2490	K_T	0.0370	0.6158
R^2	0.9312	0.9241	mT	0.8409	0.0827
SSE	9.8646	12.4238	R^2	0.9787	0.9320
RMSE	39.4587	49.6951	SSE	3.0524	11.1336
			RMSE	9.1572	33.4008
Dubinin-Radushkevich			Khan		
			q_k (mg/g)	67.2035	2.549
q_D (mg/g)	189.36138	146.023	b_k	0.0158	0.4534
E_s (kJ/mol)	0.6112	0.9242	a_k	1.1660	2.2856
R^2	0.9396	0.9017	R^2	0.9787	0.9999
SSE	8.6502	20.1468	SSE	3.0635	0.0020
RMSE	34.6007	80.5872	RMSE	9.1904	2.0110

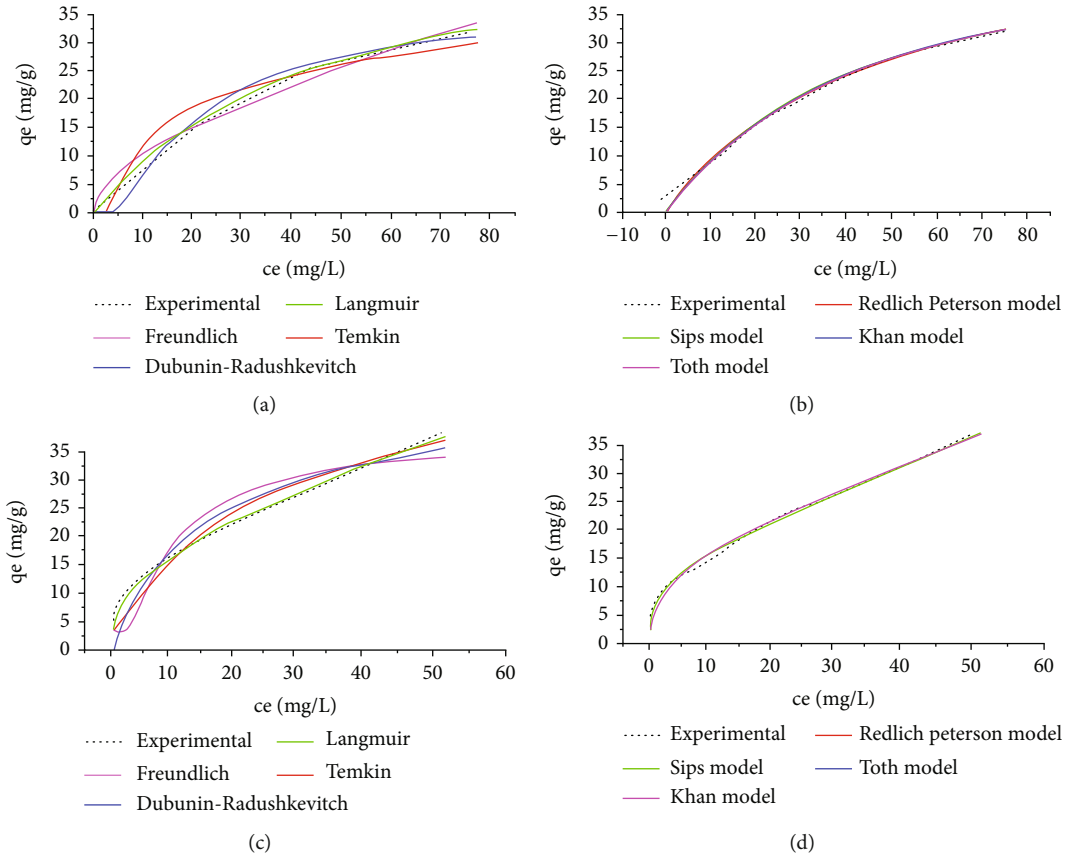

Figure 11: Adsorption isotherm of two-parameter and three-parameter models of Red 2BN adsorption on (a, b) JPAC and (c, d) JPAC/TiO_2 adsorbents.

Table 6: Intraparticle diffusion rate parameter and diffusion coefficient for the adsorption of Red 2BN on JPAC and JPAC/TiO_2.

C_0 (mg/L)	JPAC				JPAC/TiO_2			
	K_{id} (mg/g.min$^{0.5}$)	$D_1 \times 10^{10}$ (m^2/s)	$D_2 \times 10^{12}$ (m^2/s)	D_e (m^2/s)	K_{id} (mg/g.min$^{0.5}$)	$D_1 \times 10^{10}$ (m^2/s)	$D_2 \times 10^{12}$ (m^2/s)	D_e (m^2/s)
25	0.2425	3.9631	0.8152	0.6761	0.24279	3.964	0.7015	0.5961
50	0.4597	3.9850	1.0124	0.8073	0.4949	4.0018	0.5636	0.4940
100	0.8420	3.9040	0.8323	0.6860	0.8988	3.9038	0.634	0.5454
200	1.4994	3.7201	0.9349	0.7472	1.7413	3.9191	0.7145	0.6043
300	2.2001	3.7201	1.3345	0.9822	2.5591	3.9495	0.7145	0.6050
400	3.0743	3.9289	1.0859	0.8508	3.2707	3.8940	0.7145	0.6037

In addition to that, the higher negative values of ΔG° direct the powerful auspicious adsorption process [46, 47]. Also, in which ΔS° tends to be negative [48] following free energy values suggests that Red 2BN molecules were physisorbed onto active sites of JPAC and JPAC/TiO_2. It also proposes that Red 2BN molecules on the surface lead to the interaction of H-bonding, dipole-dipole interaction, or electrostatic tie-up [6].

The extent of adsorption of Red 2BN dye molecules onto the surface of JPAC and JPAC/TiO_2 was revealed by considering the effect of contact time (4 h), initial concentration (400 mg/L), pH, carbon loading (0.5 g), and temperature (303 K). Table S1 shows a comparison of adsorption capacity with other papers using biomass as source to AC preparation to treat synthetic dyes.

3.3. Kinetic Studies. To scrutinize the kinetics of Red 2BN molecules onto the sites of JPAC and JPAC/TiO_2, the experimental data of kinetic models are given in Table 4. Using kinetic expressions, kinetic rate constants (k_1 and k_2), initial sorption rate, and calculated adsorption capacity (q_e) were predicted and compared for both adsorbents. From the table, a very low value of R^2 was observed for the pseudofirst-order model as well as for the Elovich model. However, higher values of R^2 were observed (>0.99 in both cases) for type I expression at all initial dye concentrations

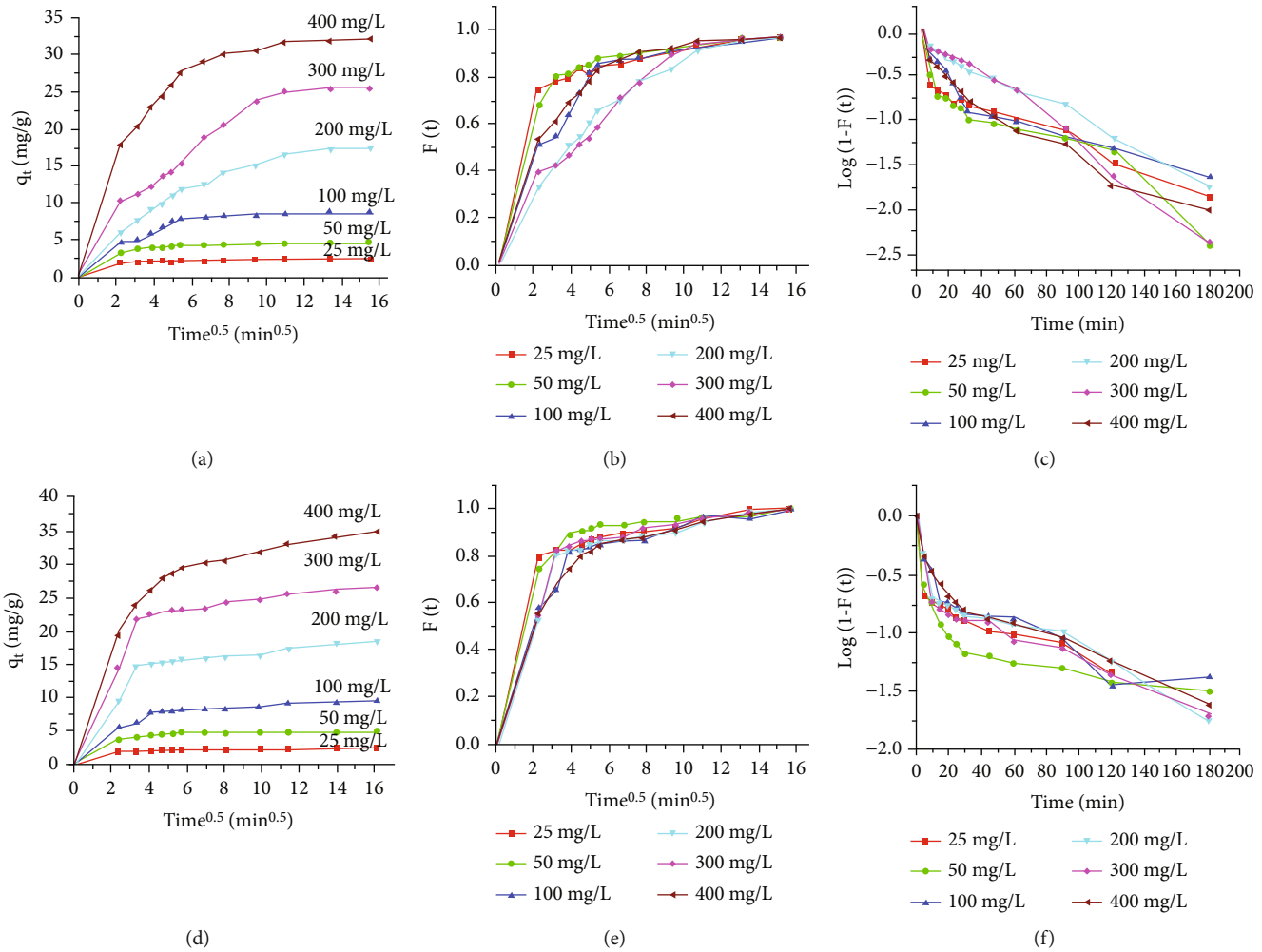

Figure 12: Intraparticle diffusion plot of Red 2BN on adsorbents of (a–c) JPAC and (d–f) JPAC/TiO_2 adsorption process.

suggest that the pseudosecond-order kinetic expression fits well for the optimum uptake of Red 2BN molecules on JPAC and JPAC/TiO_2. In addition to that, the calculated adsorption capacity (q_e) was nearer to the experimental q_e but in the case of the pseudofirst-order, it deviates to have a poorer value. And increasing the initial concentration, the uptake capacity of Red 2BN molecules declined to values for both adsorbents which are experimentally and practically impossible. Convincingly Red 2BN/activated carbon system fits well for type I linear pseudosecond-order expression, and it gets violated in the case of pseudofirst-order for the same experimental data. Similarly, the kinetic plot of the pseudosecond-order model of JPAC and JPAC incorporated TiO_2 is shown in Figure 10.

The initial sorption rata (h) gets increased when concentration proceeds higher but for fewer cases, it deviates. Also, the desorption constant (β) getting decreased by increasing the concentration suggests the competition of Red 2BN molecules complex at high concentrations.

3.4. Isotherm Studies. Generally, adsorption isotherm explains the nature of adsorbents and how well the adsorbates interact with the adsorbent surface. Herewith, the adsorption isotherm of the two-parameter and three-parameter models was studied for JPAC and JP incorporated TiO_2 adsorbents which are tabulated in Table 5. The linear method shows inherent bias, and to overcome these issues, nonlinear method was used to corroborate the model through MATLAB 2015a. Indeed, more number of parameters in equation shows lesser error function by considering all errors occur during experiments [49]. Comparing with the results in Table 5, considering the two-parameter model, Langmuir's isotherm fits well for both JPAC and JPAC/TiO_2 utilizing and linking the coefficient of regression (R^2), sum of square errors (SSE), and root mean square error (RMSE). Also, in Langmuir isotherm, a dimensionless separation factor (R_L) tends to represent a value of $R_L = 0.6579$ for JPAC and TiO_2 incorporated JPAC $R_L = 0.5442$ suggests the adsorption of Red 2BN molecules was favorable. Similarly, Freundlich and D-R model tells the adsorption process was favorable by physical mechanism further confirms from the value of $n = 1.6915$, Es = 0.6112 kJ/mol for JPAC and JPAC/TiO_2 $n = 1.7937$, Es = 0.9242 kJ/mol suggest the nature of adsorption was the physical mode by attaching the Red 2BN molecules on active sites through energetically identical monolayer sorption process. In addition, the maximum

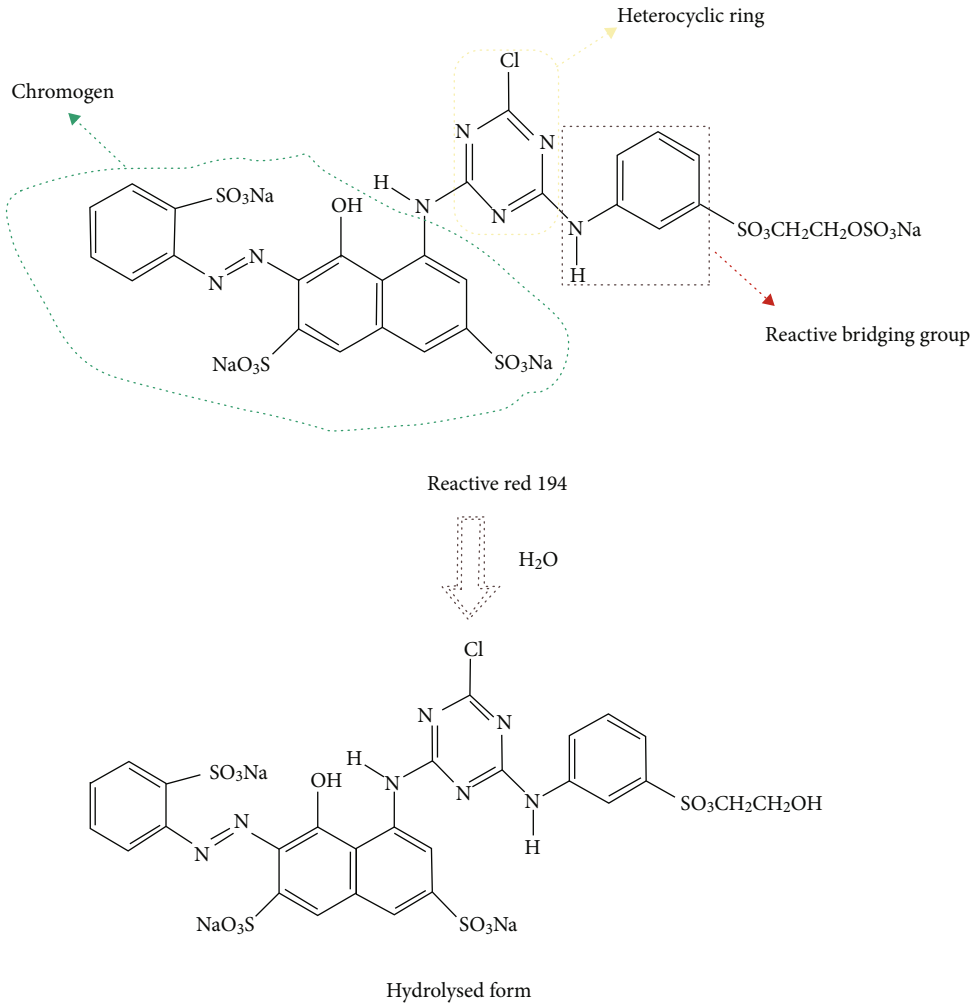

Figure 13: Nature of azo dyes during hydrolysis.

monolayer adsorption capacity of $q_L = 52.6$ (mg/g) for JPAC and $q_L = 53.20$ (mg/g) for JPAC/TiO_2 was noted. As in the case of the three-parameter model, the Khan isotherm model fits well for JPAC/TiO_2 by considering their R^2 value to be higher compared with other models; in addition to that, the SSE and RMSE values are lower compared with other fits. Again, it tells the adsorption is Langmuir with the value of constant mT is greater than one. But in the case of JPAC, Sips isotherm fits well through the values of R^2, SSE, and RMSE and suggests that it follows Langmuir adsorption by the constant of m is equal to one. Assembling the results, isotherm suggests that the sorption of Red 2BN molecules on the surface of active sites was monolayer. Figures 11(a)–11(d) depict a nonlinear plot of both adsorbents of two-parameter and three-parameter models that fits well with experimental data.

3.5. Adsorption Mechanism

3.5.1. Diffusion Model of Red 2BN Dye on Jackfruit Peel Activated Adsorbents. The adsorption mechanism is majorly governed by guessing the rate-limiting step which in turn calls for design drives. In the case of the solid-liquid adsorption process, a molecular exchange is generally commented on by either boundary layer diffusion (external mass transfer) or intraparticle diffusion or both. The most commonly used technique for observing the adsorption mechanism by fitting experimental data with the intraparticle diffusion model is given in Table 6. The plot of qt versus $t0.5$ for the adsorption of Red 2BN molecules on JPAC and JPAC/TiO_2 is shown in Figures 12(a)–12(c) and 12(d)–12(f). From the figure, Red 2BN molecular adsorption follows two distinct trends that confirm the adsorption process proceeded by both film diffusion (D_1) and pore diffusion (D_2). By assuming the conditions in Fick's law, the diffusion coefficients of both D_1 and D_2 were calculated which helps to find effective diffusion coefficients. The straight line does not pass through the origin which further confirms the nature of both film diffusion, as well as intraparticle diffusion, occurred by a rapid step follows a gradual uptake of Red 2BN molecule onto the surface voids of JPAC and JPAC/TiO_2. By the plot, the slope of the second linear portion gives an intraparticle diffusion rate constant K_{id}. Further, the contribution of film diffusion to be the rate-limiting step once the intercept becomes larger when the concentration gets increases. The kinetic adsorption data were further analyzed by the

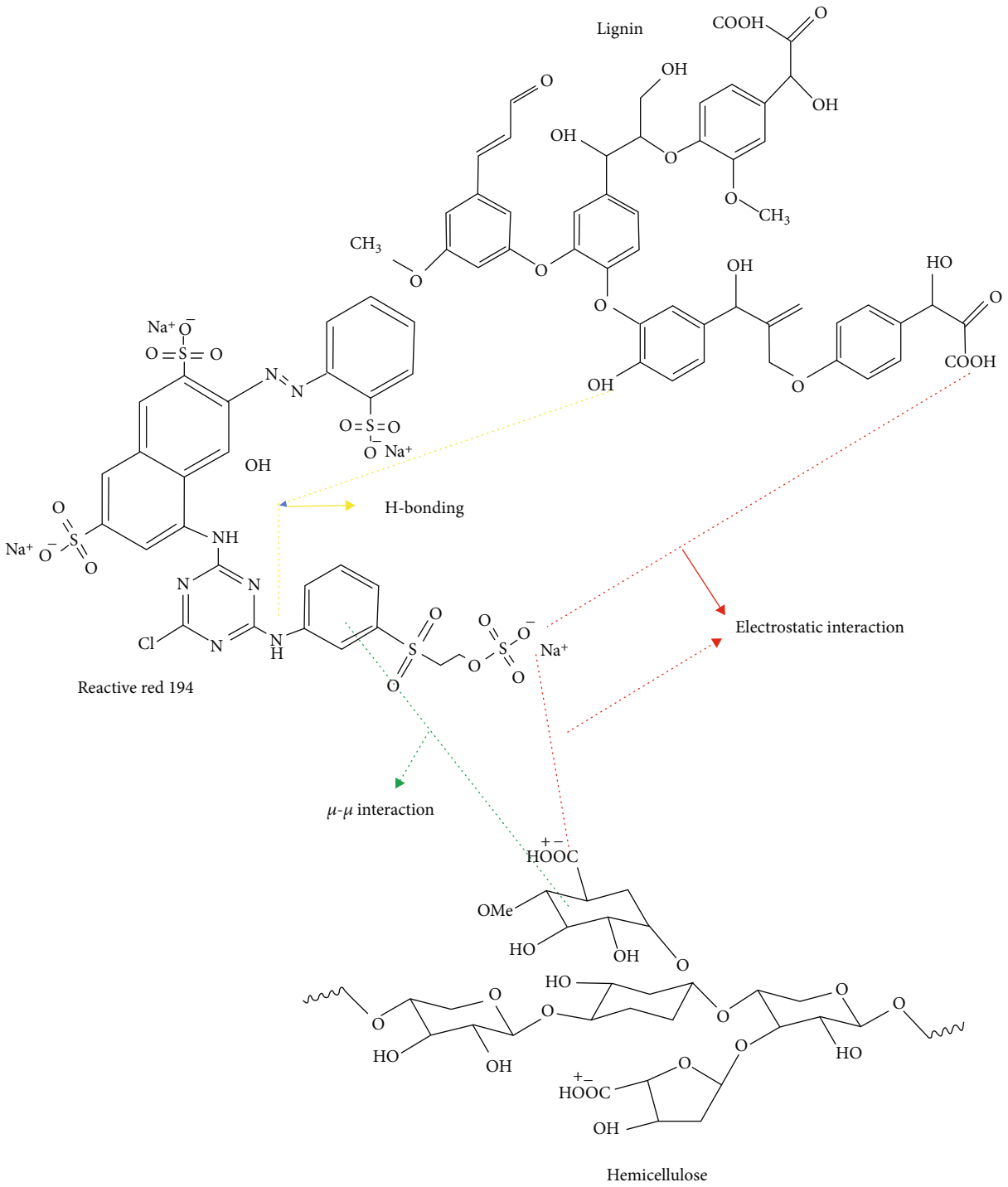

Figure 14: Illustrative representation of Red 2BN on active sites of adsorbents.

procedure given by Reichenberg [32] and Helfferich [33] to establish the rate-limiting step of Red 2BN onto the sites of JPAC and JPAC/TiO_2. A linear plot B_t vs. t was used to distinguish between the film diffusion and particle diffusion for different initial concentrations on active sites. At low concentrations, the storyline is not original; this shows that film diffusion is the speed control setting. Either way, at higher concentrations, the B_t vs. t plot moves towards the origin, which indicates the diffusion of the particles to be controlled. Herein, multilinear plots of adsorption stages were found for three conditions of lower, moderate, and longer regimes for getting D_1, D_2, and D_e.

3.5.2. Proposed Scheme of Red 2BN ($C_{27}H_{18}ClNa_4O_{16}S_5$) on Adsorbents. Azo dyes have a functional group of N=N with aromatic ring structures that frame the largest group of synthetic dye which constitutes two groups of monocholorotriazine and vinyl sulphone types. This type of dye carries one

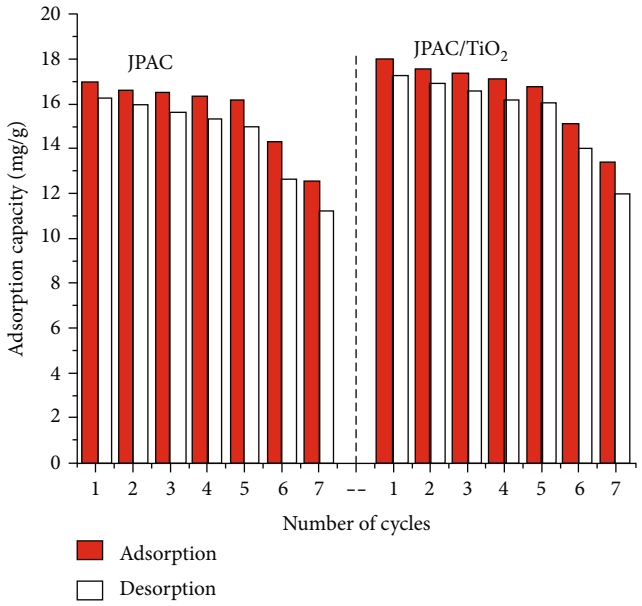

Figure 15: 2-D plot of adsorption desorption progression cycles on JPAC and JPAC/TiO_2 on different runs.

Table 7: Characteristics of waste water.

Characteristics	Predicted values of raw effluent	Permissible limit
Hardness	675 mg/L	250 mg/L
COD	32000 mg/L	120 mg/L
Suspended solids	1700 mg/L	50 mg/L
Dissolved solids	42340 mg/L	2000 mg/L
pH	6.5	6-9

chlorine and 5 sulfur atoms in its structure having a reacting bridging group that tends to attach the mandatory charge of other molecules of opposite charge. By generating phosphate bonds, phosphoric acid aids in the formation of a bridge that joins fragments of biopolymers, opening pores, and increasing the surface area of the carbon sample. It demonstrates that phosphoric acid is an effective activator for lignocellulosic biomasses. However, large concentrations of phosphoric acid may cause porous structural degeneration due to severe dehydration with additional acid. So this is aimed at forming cross-interconnected pores of straight uniform tubes are evident for the passage of reacting groups of dye to adhere in Figure 6(a). Similarly in Figure 7, pores with adhered molecules of TiO_2 on surface tend to seize the dye. The pore formation was confirmed by SEM analysis. In Figures 6(b) and 7(b), all the pores are blocked by the Red 2BN molecule resembles like a smooth surface. This happens because the primary state of adsorption at empty surface sites is available, and after equilibrium is achieved, the remainder of the vacant sites is difficult to be ideal and may be wedged by repulsive interactions between dye molecules. From FTIR analysis, the group formation of meta and parasubstituted benzene group and C-H aromatic groups after adsorption resembles the reactive dye portion.

Here in Figure 13, the nature of dyes is specified with their reactivity and the bridging group for the attachment on active sites was understood pictorially in a similar fashion; the molecules of Red 2BN get attached during hydrolysis. The red box in Figure 13 is responsible for the accessory part of their associated charges. The green color loop is the coloring agent of dye call chromogen which is unreactive, and during the process, only the reacting species are friendly to active sites. To make a further clear view, Red 2BN molecules can be attached on the active sites of prepared adsorbents are embodied in Figure 14 as proposed pathway scheme.

3.6. Desorption Studies. Contemporary revival of spent adsorbents on the adsorption process was essentially decisive in hands-on applications. To study the repeatability of carbon, desorption experiments were performed under batch mode to forecast the desorption efficiency. The Red 2BN-loaded JPAC and JPAC/TiO_2 composite was eluted by using different desorbing agents (0.1 M HCl, 0.1 M NaOH, and distilled water) to evaluate the reusability of the Red 2BN-loaded adsorbents. The Red 2BN-loaded JPAC and JPAC/TiO_2 were agitated with the eluents for the same duration as that of the reaction time (4 h) [24]. After each treatment, the adsorbent material was separated from the dye solution and washed with distilled water. After filtration, the solid residue was again agitated with the fresh 50 mL Red 2BN solution (50 mg/L) for another cycle.

It can be observed from figure S1 that the use of distilled water shows prominent dye desorption efficiency because of the nature of Red 2BN as the reactive dye has enhanced dispersible essence which is readily soluble in water makes the molecular bombardment tends to eject the physisorbed Red 2BN molecules present in the active sites. The uses of other desorbing agents are HCl (0.1 M) and NaOH (0.1 M) which shows lesser desorption efficiency on both JPAC and JPAC/TiO_2. More H^+ are generated from the solution thus results in prime a competition between the cationic exchanges of Red 2BN molecules with the usage of an acidic desorbing agent. Moreover, the use of a base desorbing agent corresponds to form precipitates, and also, uptake is insignificant at lower pH from the solution gives lesser molecular randomness compared to distilled water [24]. A comparatively enormous amount of Red 2BN molecules desorbed from distilled water can be explained due to the protonation of both H^+ and OH^- which results in the electrostatic repulsion of molecules from the active sites [50]. So, further studies follow with the distilled water. The amount of Red 2BN desorbed (% desorption) in each case was computed by using the following relationship.

$$\%\text{Desorption} = \frac{\text{concentration of desorption}}{\text{concentration of adsorption}}, \quad (9)$$

where C_{des} and C_{ads} (mg/L) represent the concentration of dye in desorbed and adsorbed phases, respectively. The adsorbent material was separated from the Red 2BN solution and filtered off to decant the solid residue for the next cycle.

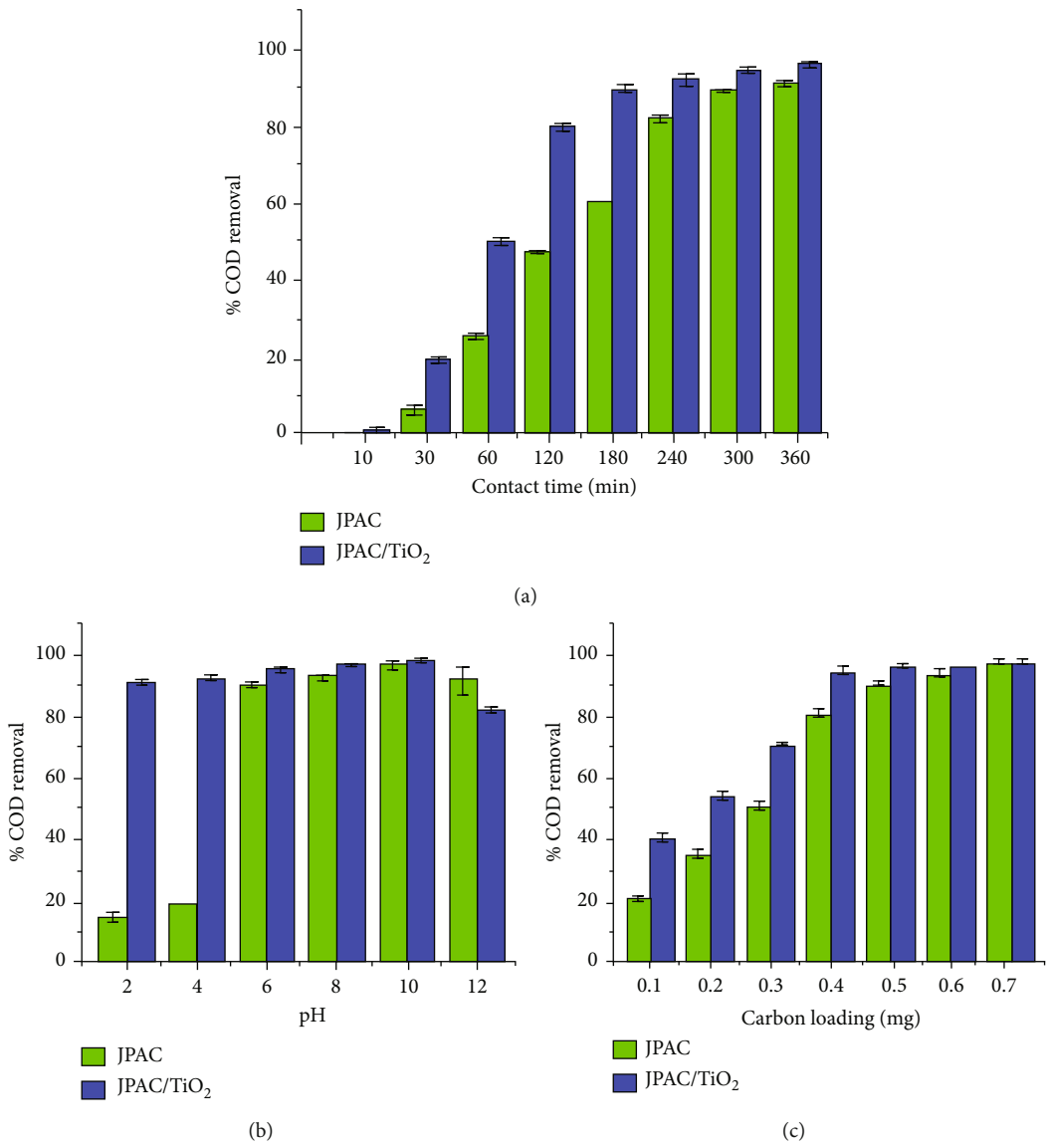

Figure 16: Effect of (a) contact time, (b) pH, and (c) carbon loading on COD removal using JPAC and JPAC/TiO_2 for tannery effluents (adsorbent dose = 0.5 g, COD C_i = 4000 mg/L, solution pH, T = 303 K, and contact time = 4 h).

Table 8: Typical parameters of tannery effluent (Red 2BN) before and after adsorption.

Parameters	Constituents present in tannery effluent (Red 2BN) before adsorption	Constituents present in tannery effluent (Red 2BN) after adsorption		Permissible limits for discharging the water to the ecosystem
		JPAC	JPAC/TiO_2	
pH	6.5	6.1	6.1	6-9
Suspended solids (mg/L)	50	32	25	50
Dissolved solids (mg/L)	5290	1518	1494	2000
BOD (mg/L)	514	37	23	100
COD (mg/L)	4000	94.830	63.200	120

3.6.1. Progression of Adsorption Desorption Cycles. Repeated revolution of adsorbents could be estimated by a series of sequences that could be done in the same order of adsorption-desorption studies. In which an excellent performance of adsorbents shows glowing in adsorption as well as desorption processes which will minimize the secondary pollution and operational cost. To follow up with the two-dimensional outcomes shown in Figure 15, JPAC/TiO_2 has a strong potential to adsorb a significant amount of Red 2BN molecules from the aqueous region compared to the

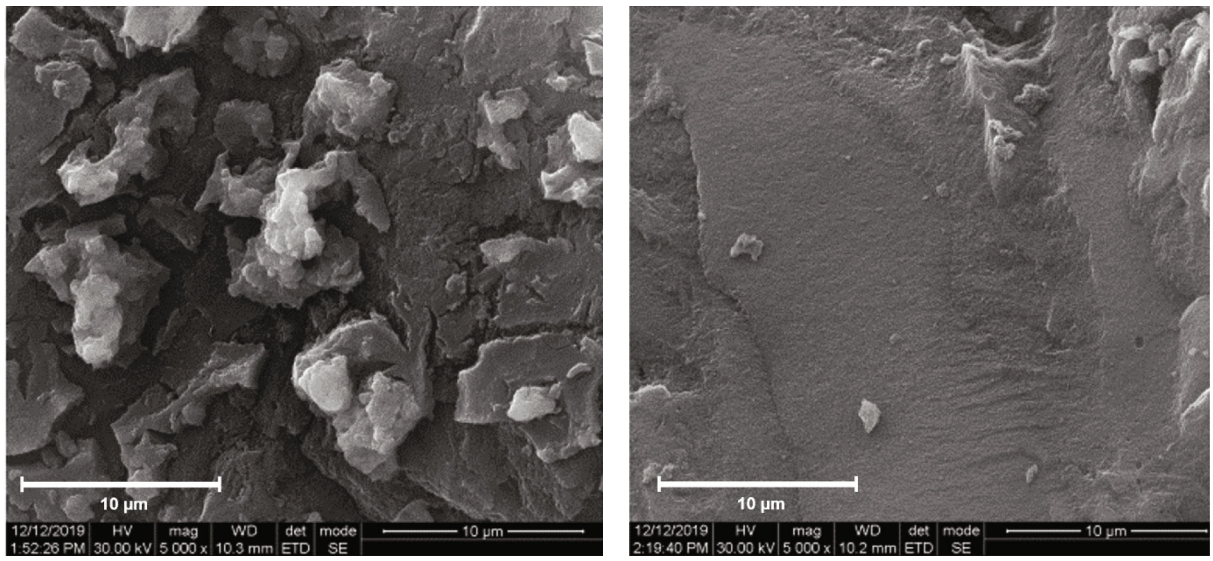

(a) (b)

Figure 17: SEM morphology of biochar (a) JPAC and (b) JPAC/TiO_2 after adsorption of tannery effluent.

counterpart (JPAC) when it tends to do the repeated succession. Substantially, a small decrease from 17.92 mg/g (cycle 1) to 16.89 mg/g (cycle 7) of adsorption capacity of Red 2BN molecules on JPAC/TiO_2 was profound during reproducibility study in contrast with the adsorption capacity of JPAC shows 16.97 mg/g (cycle 1) to 15.07 mg/g (cycle 7) with aid of desorbing agent distilled water. This shows the desorption efficiency of JPAC/TiO_2 (≥93.4) is slightly higher compared to JPAC (≥89.2). Connecting to the above prediction, also the Gibbs free energy value predicts the nature of adhered molecules on the surface. Red 2BN molecular sorption onto the surface via physisorption process ($\Delta G = -4.17$ kJ/mol) in case of JPAC/TiO_2 could be easily detached through continuous contact of distilled water at 150 rpm for 4 h but with the counterpart of JPAC $\Delta G = -3.50$ kJ/mol likely to be slightly tougher for desorption, so that the Red 2BN molecules of weaker interactions get discharged easily from JPAC/TiO_2 compared to JPAC.

3.7. Real Effluents. The tannery effluent containing Red 2BN dye was collected from the Tannery Division of CLRI, Chennai. The samples were stored in glass bottles and kept carefully in a deep freezer for further analysis. Wastewater discharge from the leather industry varies from plant to plant depending upon the process they preferred. Here they have a process of soaking I and II followed by paint liming, reliming, washing, deliming, washing, pickling, and finally by chrome tanning. In the effluent treatment section, this raw wastewater had undergone the primary and secondary treatment followed by the awaiting process of adsorption treatment as a tertiary stage. The real effluent was dark blackish-red with a self-same pungent odor.

There were so many parameters influencing the wastewater such as chemical oxygen demand (COD), biological oxygen demand (BOD), suspended solids (SS), dissolved solids (DS), pH, and hardness. Formerly, the collected samples were characterized to check the limits of permissible nature of effluent, and those typical parameters are listed in Table 7; here all the parameters are higher than the permissible limits which were considered as toxic to aquatic life and human so that it needs a treatment to trim down the level of toxicity before discharge to the ecosystem.

A batch adsorption study was carried out in the commercially available form of reactive (Red 2BN) azo dye and fixed the optimum conditions. To proceed further with the real effluent, optimum conditions were fixed from the synthetic dye as a base for choosing the initial concentration of real effluent. In a similar fashion, the selected effluent was influenced by different operating parameters such as contact time, carbon loading, and pH to study the percentage removal of COD. To start up the COD analysis, the initial COD concentration (COD C_i) of 4000 mg/L was taken with specified conditions (solution pH, contact time = 4 h, carbon loading = 0.5 g, and $T = 303$ K) which are depicted in Figure 16.

Table 8 represents the target values for the removal of COD where 120 mg/L is to be considered as final after adsorption process as well the addition of activated carbon to the wastewater does not change the nature of pH. In a quite similar way as in synthetic wastewater, the level of COD gets reduced in real effluent over a contact time represents more active sites to bind the molecules on the surface of both JPAC and JPAC/TiO_2. The COD values of real effluent trim down within the permissible limits of JPAC (97%) and JPAC/TiO_2 (98%), respectively, which is much more appreciable. And the other parameters are reduced within the permissible limits which are shown in Table 8. On treatment with the adsorbents, the color of effluent becomes colorless with a little pinch of turbid and the highly disgusting odor gets reduced completely. Concisely, the optimum loading of carbon required for the treatment of wastewater without dilution for 4 h with a condition of solution pH under

room temperature is reliable for large scaleup. To confirm further with the active sites of both adsorbents, SEM images of adsorbent after treatment are depicted in Figures 17(a) and 17(b). It reveals that the surface gets blocked completely by the Red 2BN molecules without any voids on the image was seen. However, the adsorbents (JPAC and JPAC/TiO_2) perform well for both synthetic and real effluents, and Red 2BN molecules conceded in adsorbents.

3.8. Feasibility Study on Adsorption Performance of Jackfruit Peel. India is the second biggest producer of the jackfruit (Artocarpus heterophyllus) tree of the mulberry family (Moraceae) is originated in the south-western rain forests of India and is considered as the motherland of jackfruit. In India, it has wide distribution from Assam, Tripura, Bihar, Uttar Pradesh, the foothills of the Himalayas and South Indian States of Kerala, Karnataka, and Tamilnadu. Specifically, Tamilnadu produced 49,737 tonnes of jackfruit every year, and Cuddalore District alone contributes 60.42 metric tonnes. Merely 30 to 35% of the matured jackfruit is considered as waste includes peels, rinds, pulps, and cores except the other value-added products such as fruits and seeds. This study is to convert the jackfruit peels and small number of rinds into a valuable activated carbon of initially 50 grams of peel gives a yield of around 38 grams of activated carbon. In the same way, 23.38 tonnes of activated carbon could be prepared from the sources near Cuddalore District and can be utilized as an adsorbent in treating the industrial wastewaters. To scale up the production of activated carbon from JP for larger volumes of wastewater treatment in industries was possible as well as it deserves to be a recyclable technique.

4. Conclusion

Biosorbents are synthesized from jackfruit peels that are ideally used as an adsorbent for adsorbing the Red 2BN dye from tannery effluent wastewater. TGA, FTIR, BET, and SEM/EDX were used to characterize the adsorbent. Adsorption performance is improved by introducing the JPAC/TiO_2 dose. This can be attributed to the huge surface area and more available adsorption sites. According to the results, the process of adsorption is quite slow at the primary stage based on the available vacant surface sites are typically ideal and are repulsively impacted by the interactions between the dye molecules and vacant sites. This can be attributed to the huge surface area and the availability of many adsorption sites. Under ideal experimental settings, eco-friendly JPAC and JPAC/TiO_2 could remove dye by 97 percent and 98 percent, respectively, in a four-hour batch experiment at pH 6.5 and room temperature. The Red 2BN adsorption behavior of the peel JPAC was well matched in terms of the Langmuir isotherm, with the optimal adsorption capacity of 49.7 mg/g, while pseudosecond order could explain the kinetic data. It can be concluded that the prepared biosorbents are a viable and environmentally acceptable option for large production and could be used to remove Red 2BN from tannery effluent.

Data Availability

All data generated or analyzed during this study are included in this published article.

Conflicts of Interest

The authors declare that they have no conflicts of interest.

Authors' Contributions

The authors contributed to the study conception and design. Material preparation, data collection, and analysis were performed by Lavanya Ramasamy. The first draft of the manuscript was written by Lavanya Ramasamy. Review and supervision was performed by Dr. Lima Rose Miranda.

Supplementary Materials

(1) Proximate analysis of adsorbent. (2) Two-parameter model. (3) Three-parameter model. (4) Error functions. (5) Table S1: comparison of other adsorbents in literature. (6) Figure S1: consequence of desorbing agent on JPAC and JPAC/TiO_2 adsorbents after adsorption. *(Supplementary Materials)*

References

[1] B. H. Hameed, "Removal of cationic dye from aqueous solution using jackfruit peel as non-conventional low-cost adsorbent," *Journal of Hazardous Materials*, vol. 162, no. 1, pp. 344–350, 2009.

[2] M. R. Sohrabi and M. Ghavami, "Photocatalytic degradation of Direct Red 23 dye using UV/TiO2: effect of operational parameters," *Journal of Hazardous Materials*, vol. 153, no. 3, pp. 1235–1239, 2008.

[3] M. Abbasi and N. Razzaghi-Asl, "Sonochemical degradation of Basic Blue 41 dye assisted by nanoTiO2and H2O2," *Journal of Hazardous Materials*, vol. 153, no. 3, pp. 942–947, 2008.

[4] B. Lodha and S. Chaudhari, "Optimization of Fenton-biological treatment scheme for the treatment of aqueous dye solutions," *Journal of Hazardous Materials*, vol. 148, no. 1-2, pp. 459–466, 2007.

[5] M. A. Behnajady, N. Modirshahla, and F. Ghanbary, "A kinetic model for the decolorization of C.I. Acid Yellow 23 by Fenton process," *Journal of Hazardous Materials*, vol. 148, no. 1-2, pp. 98–102, 2007.

[6] M. Helen Kalavathy and L. R. Miranda, "Moringa oleifera-a solid phase extractant for the removal of copper, nickel and zinc from aqueous solutions," *Chemical Engineering Journal*, vol. 158, no. 2, pp. 188–199, 2010.

[7] M. H. Kalavathy and L. R. Miranda, "Comparison of copper adsorption from aqueous solution using modified and unmodified Hevea brasiliensis saw dust," *Desalination*, vol. 255, no. 1-3, pp. 165–174, 2010.

[8] D. Prahas, Y. Kartika, N. Indraswati, and S. Ismadji, "Activated carbon from jackfruit peel waste by H3PO4 chemical activation: pore structure and surface chemistry characterization," *Chemical Engineering Journal*, vol. 140, no. 1-3, pp. 32–42, 2008.

[9] I. Anastopoulos and G. Z. Kyzas, "Agricultural peels for dye adsorption: a review of recent literature," *Journal of Molecular Liquids*, vol. 200, pp. 381–389, 2014.

[10] I. Anastopoulos, I. Pashalidis, A. Hosseini-Bandegharaei et al., "Agricultural biomass/waste as adsorbents for toxic metal decontamination of aqueous solutions," *Journal of Molecular Liquids*, vol. 295, article 111684, 2019.

[11] A. Demirbas, "Agricultural based activated carbons for the removal of dyes from aqueous solutions: a review," *Journal of Hazardous Materials*, vol. 167, no. 1-3, pp. 1–9, 2009.

[12] B. S. Inbaraj and N. Sulochana, "Carbonised jackfruit peel as an adsorbent for the removal of Cd (II) from aqueous solution," *Bioresource Technology*, vol. 94, no. 1, pp. 49–52, 2004.

[13] B. S. Inbaraj and N. Sulochana, "Use of jackfruit peel carbon (JPC) for adsorption of rhodamine-B, a basic dye from aqueous solution," *Indian Journal of Chemical Technology*, vol. 13, pp. 17–23, 2006.

[14] Y. Li, X. Li, J. Li, and J. Yin, "TiO_2-coated active carbon composites with increased photocatalytic activity prepared by a properly controlled sol-gel method," *Materials Letters*, vol. 59, no. 21, pp. 2659–2663, 2005.

[15] Y. Li, S. Zhang, Q. Yu, and W. Yin, "The effects of activated carbon supports on the structure and properties of TiO 2 nanoparticles prepared by a sol-gel method," *Applied Surface Science*, vol. 253, no. 23, pp. 9254–9258, 2007.

[16] L. Yan, S. Hu, and C. Jing, "Recent progress of arsenic adsorption on TiO2 in the presence of coexisting ions: a review," *Journal of Environmental Sciences (China)*, vol. 49, pp. 74–85, 2016.

[17] L. Cao, D. Xie, Y. Qu, and C. Jing, "Preparation of activated carbon (AC)-loaded TiO 2 adsorbent," *Rare Metals*, vol. 30, no. S1, pp. 217–220, 2011.

[18] S. H. Ranasinghe, A. N. Navaratne, and N. Priyantha, "Enhancement of adsorption characteristics of Cr (III) and Ni (II) by surface modification of jackfruit peel biosorbent," *Journal of Environmental Chemical Engineering*, vol. 6, no. 5, pp. 5670–5682, 2018.

[19] T. Kodom, A. Dougna, I. Tchakala, M. E. D. Gnazou, G. Djaneye-Boundjou, and M. L. Bawa, "TiO 2 PC500 coated on non woven paper with SiO 2 as a binder-assisted photocatalytic degradation of reactive black 5 in aqueous solution," *Journal of Water Resource and Protection*, vol. 5, pp. 1227–1234, 2013.

[20] Y. Li, X. Zhou, W. Chen et al., "Photodecolorization of Rhodamine B on tungsten-doped TiO 2/activated carbon under visible-light irradiation," *Journal of Hazardous Materials*, vol. 227, pp. 25–33, 2012.

[21] T. S. Jamil, M. Y. Ghaly, N. A. Fathy, T. A. Abd el-halim, and L. Österlund, "Enhancement of TiO 2 behavior on photocatalytic oxidation of MO dye using TiO 2/AC under visible irradiation and sunlight radiation," *Separation and Purification Technology*, vol. 98, pp. 270–279, 2012.

[22] M. Arulkumar, P. Sathishkumar, and T. Palvannan, "Optimization of Orange G dye adsorption by activated carbon of Thespesia populnea pods using response surface methodology," *Journal of Hazardous Materials*, vol. 186, no. 1, pp. 827–834, 2011.

[23] M. A. Miranda, P. Dhandapani, M. H. Kalavathy, and L. R. Miranda, "Chemically activated Ipomoea carnea as an adsorbent for the copper sorption from synthetic solutions," *Adsorption*, vol. 16, no. 1-2, pp. 75–84, 2010.

[24] I. Shah, R. Adnan, W. S. W. Ngah, and N. Mohamed, "Iron impregnated activated carbon as an efficient adsorbent for the removal of methylene blue: regeneration and kinetics studies," *PLoS One*, vol. 10, no. 4, pp. 1–23, 2015.

[25] K. Y. Foo and B. H. Hameed, "Insights into the modeling of adsorption isotherm systems," *Chemical Engineering Journal*, vol. 156, no. 1, pp. 2–10, 2010.

[26] M. H. Kalavathy, I. Regupathi, M. G. Pillai, and L. R. Miranda, "Modelling, analysis and optimization of adsorption parameters for H_3PO_4 activated rubber wood sawdust using response surface methodology (RSM)," *Colloids and Surfaces B: Biointerfaces*, vol. 70, no. 1, pp. 35–45, 2009.

[27] V. R. G. Dev, J. R. Venugopal, T. S. Kumar, L. R. Miranda, and S. Ramakrishna, "Agave sisalana, a biosorbent for the adsorption of Reactive Red 120 from aqueous solution," *Journal of the Textile Institute*, vol. 101, no. 5, pp. 414–422, 2010.

[28] G. McKay, Y. S. Ho, and J. C. Y. Ng, "Biosorption of copper from waste waters: a review," *Separation and Purification Methods*, vol. 28, no. 1, pp. 87–125, 1999.

[29] M. Kisan, S. Sangathan, J. Nehru, and S. G. Pitroda, "Standard Methods of Sampling and Test (Physical and Chemical)," *Environ Prot Sect Comm CHD*, vol. 12, no. 10, 2006.

[30] J. L. F. Alves, J. C. G. da Silva, G. D. Mumbach et al., "Insights into the bioenergy potential of jackfruit wastes considering their physicochemical properties, bioenergy indicators, combustion behaviors, and emission characteristics," *Renewable Energy*, vol. 155, pp. 1328–1338, 2020.

[31] M. Jagtoyen and F. Derbyshire, "Activated carbons from yellow poplar and white oak by H_3PO_4 activation," *Carbon*, vol. 36, no. 7-8, pp. 1085–1097, 1998.

[32] A. S. Devi, M. H. Kalavathy, and L. R. Miranda, "Optimization of the process parameters for the preparation of activated carbon from low cost Phoenix dactylifera using response surface methodology," *Austin Chemical Engineering*, vol. 2, p. 1021, 2015.

[33] D. Prahas, Y. Kartika, N. Indraswati, and S. Ismadji, "The use of activated carbon prepared from jackfruit (Artocarpus heterophyllus) peel waste for methylene blue removal," *Journal of Environmental Protection Science*, vol. 2, pp. 1–10, 2008.

[34] A. M. Puziy, O. I. Poddubnaya, A. Martínez-Alonso, F. Suárez-García, and J. M. D. Tascón, "Surface chemistry of phosphorus-containing carbons of lignocellulosic origin," *Carbon*, vol. 43, no. 14, pp. 2857–2868, 2005.

[35] A. M. Puziy, O. I. Poddubnaya, A. Martínez-Alonso, F. Suárez-Garcıa, and J. M. D. Tascón, "Synthetic carbons activated with phosphoric - acid I. Surface chemistry and ion binding properties," *Carbon*, vol. 40, no. 9, pp. 1493–1505, 2002.

[36] A. Eshaghi, S. Hayeripour, and A. Eshaghi, "Photocatalytic decolorization of reactive red 198 dye by a TiO2-activated carbon nano-composite derived from the sol-gel method," *Research on Chemical Intermediates*, vol. 42, no. 3, pp. 2461–2471, 2016.

[37] J. Coates, *Interpretation of infrared spectra, a practical approach*, John Wiley & Sons Ltd, Chichester, 2000.

[38] M. A. Al-Ghouti and D. A. Da'ana, "Guidelines for the use and interpretation of adsorption isotherm models: a review," *Journal of Hazardous Materials*, vol. 393, article 122383, 2020.

[39] B. Xing, C. Shi, C. Zhang et al., "Preparation of TiO2/activated carbon composites for photocatalytic degradation of RhB under UV light irradiation," *Journal of Nanomaterials*, vol. 2016, Article ID 8393648, 10 pages, 2016.

[40] A. M. M. Vargas, C. A. Garcia, E. M. Reis, E. Lenzi, W. F. Costa, and V. C. Almeida, "NaOH-activated carbon from flamboyant (Delonix regia) pods: optimization of preparation conditions using central composite rotatable design," *Chemical Engineering Journal*, vol. 162, no. 1, pp. 43–50, 2010.

[41] T. Senthilkumar, R. Raghuraman, and L. R. Miranda, "Parameter optimization of activated carbon production from agave sisalana and punica granatum peel: adsorbents for C.I. reactive orange 4 removal from aqueous solution," *Clean-Soil, Air, Water*, vol. 41, no. 8, pp. 797–807, 2013.

[42] M. H. Kalavathy, T. Karthikeyan, S. Rajgopal, and L. R. Miranda, "Kinetic and isotherm studies of Cu (II) adsorption onto H3PO 4-activated rubber wood sawdust," *Journal of Colloid and Interface Science*, vol. 292, no. 2, pp. 354–362, 2005.

[43] T. Pálfi, L. Wojnárovits, and E. Takács, "Mechanism of azo dye degradation in advanced oxidation processes: degradation of sulfanilic acid azochromotrop and its parent compounds in aqueous solution by ionizing radiation," *Radiation Physics and Chemistry*, vol. 80, no. 3, pp. 462–470, 2011.

[44] T. Senthilkumar, S. K. Chattopadhyay, and L. R. Miranda, "Optimization of activated carbon preparation from pomegranate peel (Punica granatum Peel) using RSM," *Chemical Engineering Communications*, vol. 204, no. 2, pp. 238–248, 2017.

[45] S. Mohan and R. Gandhimathi, "Removal of heavy metal ions from municipal solid waste leachate using coal fly ash as an adsorbent," *Journal of Hazardous Materials*, vol. 169, no. 1-3, pp. 351–359, 2009.

[46] E. C. Lima, A. Hosseini-Bandegharaei, J. C. Moreno-Piraján, and I. Anastopoulos, "A critical review of the estimation of the thermodynamic parameters on adsorption equilibria. Wrong use of equilibrium constant in the Van't Hoof equation for calculation of thermodynamic parameters of adsorption," *Journal of Molecular Liquids*, vol. 273, pp. 425–434, 2019.

[47] Y. Liu, "Is the free energy change of adsorption correctly calculated?," *Journal of Chemical and Engineering Data*, vol. 54, no. 7, pp. 1981–1985, 2009.

[48] I. Tosun, "Ammonium removal from aqueous solutions by clinoptilolite: determination of isotherm and thermodynamic parameters and comparison of kinetics by the double exponential model and conventional kinetic models," *International Journal of Environmental Research and Public Health*, vol. 9, no. 3, pp. 970–984, 2012.

[49] M. Hadi, M. R. Samarghandi, and G. McKay, "Equilibrium two-parameter isotherms of acid dyes sorption by activated carbons: study of residual errors," *Chemical Engineering Journal*, vol. 160, no. 2, pp. 408–416, 2010.

[50] D. Pathania, S. Sharma, and P. Singh, "Removal of methylene blue by adsorption onto activated carbon developed from Ficus carica bast," *Arabian Journal of Chemistry*, vol. 10, pp. S1445–S1451, 2017.